CrossMark

Inter comparison of Tropical Indian Ocean features in different ocean reanalysis products

Ananya Karmakar[1,2] · Anant Parekh[1] · J. S. Chowdary[1] · C. Gnanaseelan[1]

Abstract This study makes an inter comparison of ocean state of the Tropical Indian Ocean (TIO) in different ocean reanalyses such as global ocean data assimilation system (GODAS), ensemble coupled data assimilation (ECDA), ocean reanalysis system 4 (ORAS4) and simple ocean data assimilation (SODA) with reference to the in-situ buoy observations, satellite observed sea surface temperature (SST), EN4 analysis and ocean surface current analysis real time (OSCAR). Analysis of mean state of SST and sea surface salinity (SSS) reveals that ORAS4 is better comparable with satellite observations as well as EN4 analysis, and is followed by SODA, ECDA and GODAS. The surface circulation in ORAS4 is closer to OSCAR compared to the other reanalyses. However mixed layer depth (MLD) is better simulated by SODA, followed by ECDA, ORAS4 and GODAS. Seasonal evolution of error indicates that the highest deviation in SST and MLD over the TIO exists during spring and summer in GODAS. Statistical analysis with concurrent data of EN4 for the period of 1980–2010 supports that the difference and standard deviation (variability strength) ratio for SSS and MLD is mostly greater than one. In general the strength of variability is overestimated by all the reanalyses. Further comparison with in-situ buoy observations supports that MLD errors over the equatorial Indian Ocean (EIO) and the Bay of Bengal are higher than with EN4 analysis. Overall ORAS4 displays higher correlation and lower error among all reanalyses with respect to both EN4 analysis and buoy observations. Major issues in the reanalyses are the underestimation of upper ocean stability in the TIO, underestimation of surface current in the EIO, overestimation of vertical shear of current and improper variability in different oceanic variables. To improve the skill of reanalyses over the TIO, salinity vertical structure and upper ocean circulation need to be better represented in reanalyses.

Keywords Ocean reanalyses · Indian Ocean · Error analysis

1 Introduction

Physical and dynamical features of the Tropical Indian Ocean (TIO) are different from the rest of the tropical oceans. Warm and fresh water in the Bay of Bengal (BoB) and eastern equatorial Indian Ocean are part of the Indo-Pacific warm pool. Sea surface temperature (SST) in the TIO displays strong relationship with the atmospheric convection at all the time scales (Gadgil et al. 1984) since SST is mostly close to 28 °C, which is above the threshold for atmospheric convection. Pre-monsoon Arabian Sea (AS) SST condition significantly influences the following Indian summer monsoon rainfall (ISMR, Shukla 1975). Recently Chakravorty et al. (2016) showed the changing role of the north Indian Ocean SST on ISMR variability. Seasonal and intraseasonal variability in the TIO SST is mostly driven by local air sea interaction (Schott et al. 2009; Shenoi et al. 2002; Sengupta et al. 2001), which feeds back to the atmospheric convective activity at different time scales (i.e. diurnal, intraseasonal, seasonal to inter annual, e.g., Schott and McCreary 2001; Weller et al. 2016). As the TIO is a major part of the largest warm pool over the global ocean, its interaction with the atmosphere also plays a dominant role in shaping climate

✉ Anant Parekh
anant@tropmet.res.in

[1] Indian Institute of Tropical Meteorology (IITM), Pune 411008, India

[2] Department of Atmospheric and Space Sciences, Savitribai Phule Pune University, Pune 411007, India

on regional and global scales (Xie et al. 2009; Schott et al. 2009). In addition to that the TIO surface and subsurface modes of variability in turn plays a significant role in the regional climate variability (Saji et al. 1999; Webster et al. 1999; Saji and Yamagata 2003a, b; Schott et al. 2009; Liu et al. 2014; Sayantani and Gnanaseelan 2015). In the recent years TIO also displayed strong SST thermocline coupling (Chakravorty et al. 2014).

Sea surface salinity (SSS) does play a significant role in the formation of shallow halocline in the BoB (e.g., Shetye et al. 1996) and eastern EIO. Transport of fresh water from the BoB to the AS during winter via coastal current contributes to the formation of mini warm pool over the southeastern AS during the spring season. This warm pool favors formation of monsoon onset vortex and onset of monsoon (Seetaramayya and Master 1984). Apart from this SSS plays a significant role on the formation of upper ocean stratification (Fousiya et al. 2015; Shenoi et al. 2002) and formation of barrier layer in the TIO (Agarwal et al. 2012), which inhibits mixing. Salinity structure can have strong impact on the BoB dynamical and thermal circulation through density and dynamical height variations. SSS plays a significant role on the upper ocean structure which modifies the TIO mixed layer depth (MLD). Overall SSS and MLD modify the inertia of the ocean and leads to high frequency variability in the TIO. Apart from temperature and salinity states, horizontal circulation in the TIO also displayed unique characteristics (Wyrtki 1973). Equatorial eastward surface zonal current is one of the dominant current systems in the TIO, which transports warm water towards the east and supports warming of the eastern EIO and deepens the thermocline in the east. Variability of equatorial current affects the transports of heat and salt content, which influence the formation of one of the dominant modes of variability in the TIO, the Indian Ocean Dipole (IOD, Gnanaseelan et al. 2012). Thus SST, SSS, MLD and currents influence the TIO climate and variability significantly. For reanalyses, meaningful insight can only come when the mean and variability are reproduced with good statistical skill. However detailed evaluation of the available reanalyses products for the TIO climate and variability is lacking.

Different agencies such as National Centers for Environmental Prediction (NCEP), European Centre for Medium Range Weather Forecasts (ECMWF), Geophysical Fluid Dynamics Laboratory (GFDL) and the University of Maryland produce ocean reanalysis. These reanalyses employ different types of ocean general circulation models (OGCMs) and data assimilation techniques to combine number of networks of available ocean observations in order to get a dynamically consistent ocean state. The nature of OGCM, data assimilation schemes and observations used varies from one reanalysis to the other (Table 1); hence these reanalyses data might differ substantially. These reanalyses are the only

sources of dynamically consistent three dimensional states of oceanic parameters (e.g., Toyoda et al. 2015), which are used to study the oceanic variability at different temporal and spatial scales. Some of these reanalyses are used to initialize coupled model inter-comparison project (CMIP5) decadal integrations (e.g., Taylor et al. 2012). They are also widely used to initialize coupled models for seasonal forecast (e.g., Saha et al. 2006). Balmaseda et al. (2015) reported that the ocean reanalyses differ from the observations considerably in the tropics, where model-physics and the wind variability are key factors; large differences are seen in the thermocline and MLD. Hosoda et al. (2010) showed that high vertical resolution can improve the representation of MLD and its variability. Toyoda et al. (2015) reported that MLD estimate is sensitive to the vertical discretization in the models with low resolution vertical profile leading to the underestimation of MLD. Several recent studies (Shi et al. 2015; Palmer et al. 2015; Toyoda et al. 2015) evaluated the mean as well as variability of oceanic parameters globally in these reanalyses. They concluded that the salinity from reanalyses displayed large disagreement with observations. Apart from model physics and assimilation techniques enhancement of observations from Argo and satellites, improved fresh water forcing etc. played an important role in improving the representation of salinity by reanalyses (Shi et al. 2015). Palmer et al. (2015) reported that mean features of ocean heat content in different ocean reanalyses display largest differences in the central Indian Ocean. However none of the previous studies explored the long term mean state of the TIO surface and subsurface in these reanalyses. This has motivated us to carry out the present study of comparison of reanalyses products with EN4 analysis and satellite and in-situ observations for the mean state simulation as well as its temporal variability. This study also investigated the status of the performance of data assimilation systems, the physical models, and the quality of the ocean observing system to constrain key variables of interest for the TIO. Present study also assesses the mean vertical structure of temperature, salinity and currents in different reanalyses over the TIO. Section 2 describes different ocean reanalysis used in the present study. Section 3 includes details of observations and analysis used in the present study for the comparison purpose. Section 4 describes methodology, Sect. 5 is results and discussion and Sect. 6 is summary and conclusion.

2 Ocean re-analysis studied

In the present study widely used ocean reanalysis products [i.e. global ocean data assimilation system (GODAS), simple ocean data assimilation (SODA), ocean reanalysis system (ORAS4) and ensemble coupled data assimilation (ECDA)] are considered for detailed study.

Table 1 Details of reanalyses and analysis products used in the present study

Data set	Model used	Resolution	Assimilation	Forcing	SST and SSS restoring
GODAS	MOM v3	Horizontal 1°×1° (1/3° meridional at the tropics) Vertical 29 levels in first ~500 m are 5, 15, 25, 35, 45, 55, 65, 75, 85, 95, 105, 115, 125, 135, 145,155, 165, 175, 185, 195, 205, 215, 225, 238, 262, 303, 366, 459 (~10 m resolution in first 225 m)	3D VAR	Momentum, heat, and fresh water flux from the NCEP (R2)	First layer temperature is restored to the optimal interpolation (OI-ver. 2) SST and SSS to annual SSS climatology (Huang et al. 2010)
ECDA	MOM v4	Global Tripolar grid (360 by 200), Vertical 31 levels in first ~500 m are 5, 15, 25, 35, 45, 55, 65, 75, 85, 95, 105, 115, 125, 135, 145, 155, 165, 175, 185, 195, 205, 215, 225, 236.12,250.60, 270.62,298.30, 335.68,384.63, 446.94, 524.17 (5~225, 10 m resolution, below it increasing with depth)	Ensemble Kalman Filter	Fully coupled based on CM 2.1	No (Shi et al. 2015)
ORAS4	NEMO v3	Horizontal 1°×1° with equatorial refinement (0.3). Vertical 23 levels in first ~500 m are 5.02, 15.08, 25.16, 35.28, 45.45, 55.69,66.04, 76.55, 87.27, 98.31, 109.81, 121.95, 135.03, 149.43, 165.73, 184.70, 207.42, 235.39, 270.53, 315.37, 372.96, 446.80, 540.50 (5~110, ~10 m resolution, below it increases with depth)	NEMOVAR in its 3D-var FGAT mode	Momentum, heat, and fresh water flux from the ERA	A weak (20 year time scale) relaxation to temperature and salinity climatological values from WOA 2005 is applied throughout the water column (Balmaseda et al. 2013) and SSS to 1 year
SODA	POP 2.x	Horizontal 0.25° on average (0.25°×0.4° tropics) Vertical 20 levels in first ~500 m are 5.01, 15.07, 25.28, 35.76, 46.61, 57.98, 70.02, 82.92, 96.92, 112.32, 129.49, 148.96, 171.4, 197.79, 229.48, 268.46, 317.65, 381.39, 465.91, 579.31 (5~80 ~10 m resolution, below it increases with depth)	Optimal interpolation	20CRv2 surface wind stress and variables for bulk formulae	A relaxation to WOA 2001 climatological SSS (with 3 month relaxation time scale), Temperature and salinity profiles for 10 years. (Carton and Giese 2008)
EN4 analysis	Objective analysis (Ingleby and Huddleston 2007)	Horizontal resolution is on average (1°×1°) Vertical levels are 5.02, 15.08, 25.16, 35.28, 45.45, 55.69, 66.04, 76.55, 87.27, 98.31, 109.81, 121.95, 135.03, 149.43, 165.73, 184.70, 207.42, 235.39, 270.53, 315.37, 372.96, 446.80, 540.50	–	–	The analysis will relax to climatology in the absence of any observations

2.1 Global Ocean Data Assimilation System (GODAS)

GODAS is based on the Modular Ocean Model version 3 with a three-dimensional variational (3DVAR) data assimilation scheme (Derber and Rosati 1989). It assimilates profiles of temperature and synthetic salinity. It is forced by the momentum flux, heat flux, and freshwater flux from the NCEP atmospheric reanalysis version 2 (Kanamitsu et al. 2002) with horizontal resolution 1° × 1° (1/3° meridional at the tropics) and 40 vertical levels. It provides three-dimensional ocean state and is being used to provide ocean initial conditions to the climate forecast system (CFS) for the seasonal prediction (Saha et al. 2006, 2014). More details of GODAS are provided in Table 1.

2.2 Ensemble Coupled Data Assimilation (ECDA)

The ECDA system is an ensemble-based filtering algorithm of the GFDL's coupled climate model, CM2.1 (Delworth et al. 2006). All ECDA experiments are performed with a 12-member ensemble that is used to compute state estimation (ensemble mean) and the spread of the estimate. More details about the algorithm and parameter scales can be found in Zhang and Rosati (2010). The ocean modle used is MOM4 with 1° × 1° horizontal resolution telescoping to 1/3° meridional spacing near the equator and 50 vertical levels (10 m vertical resolution in the top 220 m). The assimilation scheme is based on an Ensemble Kalman Filter under a local least squares framework with super-parallelized technique. Ocean subsurface observations of temperature, salinity from World Ocean Database (Boyer et al. 2009), and SST are assimilated to the ECDA system using covariance structures from the coupled model, where the atmosphere is constrained by an existing atmospheric reanalysis [NCEP/NCAR reanalysis 1 for 1960–1978 (Kalnay et al. 1996) and NCEP/DOE reanalysis 2 for 1979–present (Kanamitsu et al. 2002)]. The pseudosalinity profiles are assimilated to the ECDA for the periods of 1993–2002.

2.3 Ocean Reanalysis System (ORAS4)

ORAS4, a reanalysis product of ECMWF uses Nucleus for European Modelling of the Ocean (NEMO) model (Madec 2008). Three-dimensional variational assimilation (3D-Var) algorithms NEMOVAR (Courtier et al. 1994; Mogensen et al. 2012) are used to produce reanalysis of the global ocean (Table 1). It is forced by the ERA-Interim reanalysis fluxes, the horizontal resolution is 1° in the extra tropics and refined meridional resolution of 0.3° at the equator. It has 42 vertical levels with 18 of them in the first 200 m and the first level is at 5 m. A weak relaxation to temperature and salinity climatological values from the World Ocean Atlas (WOA) 2005 (Antonov et al. 2006; Locarnini et al. 2006) is

applied throughout the water column. NEMOVAR assimilates temperature and salinity profiles, and along-track altimeter-derived sea-level anomalies. In addition to the above, observed SST and global mean sea-level variations are used to modify the heat and fresh-water budget respectively. The ocean model is forced by atmospheric-derived daily surface fluxes, instead of being computed using a bulk formula within NEMO. Compared to a control ocean model simulation, ORAS4 improves the fit to observations, the interannual variability and seasonal forecast skill (Balmaseda et al. 2013). It is important to note that ORAS4 SST is restored to Reynolds SST. It is also important to note that among all reanalyses vertical levels of ORAS4 are more consistent with EN4.

2.4 Simple Ocean Data Assimilation (SODA 1.4.3)

SODA reanalysis (Carton and Giese 2008) system consists of an OGCM based on Parallel Ocean Program numeric (Smith et al. 1992), with an average 0.25° × 0.4° horizontal resolution and 40 vertical levels with 10 m spacing near the surface. Surface freshwater flux is provided by the global precipitation climatology project monthly satellite–gauge merged product (Adler et al. 2003) combined with evaporation obtained from the bulk formula used to calculate latent heat loss. It assimilates temperature and salinity profiles with optimal interpolation (Gandin 1965). The assimilation cycle is carried out every 10 days, but the corrections are introduced incrementally at every time step. A further detail about SODA is provided in Table 1. Hence the present study includes ocean reanalyses which are produced using simple data assimilation technique to most advanced technique. Details of these reanalyses are given in Table 1.

3 Observations and baseline data used for the comparison

National Oceanic and Atmospheric Administration (NOAA) Reynolds optimum interpolation (OI) SST analysis using both in situ and satellite data (Reynolds et al. 2002) is used for studying the spatial features of SST bias. Also Hadley Centre Sea Ice and SST (HadISST, Rayner et al. 2003) data products are used in the present study, which includes data received through the global telecommunications system and comprehensive ocean–atmosphere data set. However Met Office Hadley Centre EN.4.2.0 analysis [where XBT and MBT fall rate bias corrections are based on Gouretski and Reseghetti (2010)] generated by Good et al. (2013) is used (available from http://www.metoffice.gov.uk/hadobs) as a baseline. Which is based on subsurface ocean temperature and salinity profile data obtained from the World Ocean Database, global

temperature and salinity profile program, argo, and Arctic synoptic basin wide oceanography project collections. All data are subjected to a series of quality control procedures and assigned quality flags. Mainly three new checks are introduced in this version of the data set with respect to previous version (Good et al. 2013). EN4 analysis offers additional ability to make comparison over time, which further adds to create a long-term mean for the same years as for the reanalyses. Secondly EN4 analysis vertical levels are consistent with the reanalyses data. Hence the present study uses EN4 analysis monthly fields for 1980–2010 to produce monthly climatology and from it, annual climatology is produced. The root mean square differences of long term mean (1955–2012) fields of EN4 analysis and WOA is considered as an uncertainty of that particular field.

Ocean Surface Current Analyses Real-time (OSCAR) upper ocean current products based on satellite data for the period of 1993–2010 are used as observed currents for inter-comparison. OSCAR has provided unprecedented information about global ocean surface currents (~ 35 m). Sikhakolli et al. (2013) reported that over the TIO OSCAR product is able to capture the variability of the well-known surface current systems reasonably well. Study also used available monthly Research Moored Array for African–Asian–Australian monsoon analysis (RAMA, McPhaden et al. 2009) buoys observations of temperature and salinity profiles in the upper ocean. RAMA buoys observations available (Table 2) for the period 2002–2010 (or 2004–2010) are utilized to produce statistical scores. RAMA buoy first level (i.e., 1 m) observations of temperature and salinity are used to compare reanalyses first level (5 m) temperature and salinity. It is important to note that RAMA buoy observed temperature data are converted to potential temperature and used for the potential density estimates before they are compared with reanalyses.

Table 2 Details of RAMA buoys used for the intercomparison

Region	Location	Period
EIO	80.5°E, 4°S	2007–2010
	80.5°E, 1.5°S	2004–2010
	90°E, 1.5°S	2002–2010
	80.5°E, 0°	2005–2010
	90°E, 0°	2005–2010
	80.5°E, 1.5°N	2006–2010
	90°E, 1.5°N	2006–2010
	90°E, 4°N	2007–2010
	95°E, 4°N	2002–2010
BoB	90°E, 8°N	2006–2010
	90°E, 12°N	2008–2010
	90°E, 15°N	2008–2010

4 Methodology

As discussed in the previous sections, four commonly used ocean reanalyses are considered in this study for the inter-comparison with analysis/observations over the TIO. For this long term (1980–2010, 31 years) mean temperature, salinity and 1993–2010 (18 years) mean current profile data from the above reanalyses are used. Since different regions in TIO (40°E–100°E, 25°N–25°S) display specific differences, region wise comparison is also carried out (Fig. 1a) over AS (52°E–75°E, 6°N–25°N), BoB (80°E–100°E, 6°N–22°N), and EIO (40°E–100°E, 5°N–5°S). To explore the role of various processes to surface and mixed layer biases, square of the Brunt–Vaisala frequency and current shear are calculated using temperature, salinity and current profiles as follows:

Square of the Brunt–Vaisala frequency:

$$N^2 = -\frac{g}{\rho}\frac{\partial \rho}{\partial z}, \tag{1}$$

where g is the acceleration due to gravity, ρ is ocean water potential density and z is depth.

Total vertical shear of horizontal current:

$$\frac{dU}{dz}, \text{ where } U = \sqrt{u^2 + v^2}, \tag{2}$$

where U is horizontal current (m/s), u is zonal current (m/s) and v is meridional current (m/s).

Equation of state is used to estimate the role of temperature and salinity differences on the density differences

$$\Delta\rho_{temp} = -\rho_0\alpha(\Delta T),$$

$$\Delta\rho_{sal} = \rho_0\beta(\Delta S), \tag{3}$$

where, ΔT and ΔS are differences in the potential temperature and salinity with respect to EN4. Coefficients of thermal and salt expansion respectively are $\alpha = 1.7 \times 10^{-4} K^{-1}$ and $\beta = 7.6 \times 10^{-4}$.

To check the performance of the reanalyses with respect to analysis/observation statistical scores such as root mean square error (RMSE) and pattern correlation are estimated for SST, SSS, MLD and zonal and meridional currents for TIO as well as for sub regions (Table 3). To understand the seasonal evolution of RMSE, month wise RMSE analysis is also carried out. Apart from these mean features statistical scores, with concurrent samples for the period of 1980–2010 in case of SST, SSS and MLD (and 1993–2010 in the case of zonal and meridional currents) such as RMSE, standard deviation and correlation coefficient with respect to EN4 analysis are estimated and presented in tabular form (Tables 4, 5). RMSE with respect to analysis refers the root mean square difference; however RMSE with respect to observations refers error. Study also includes statistical

Fig. 1 SST (°C) biases with respect to HadISST (contour) and Reynolds SST (shaded) over the Indian Ocean from **a** GODAS **b** ECDA, **c** ORAS4 and **d** SODA
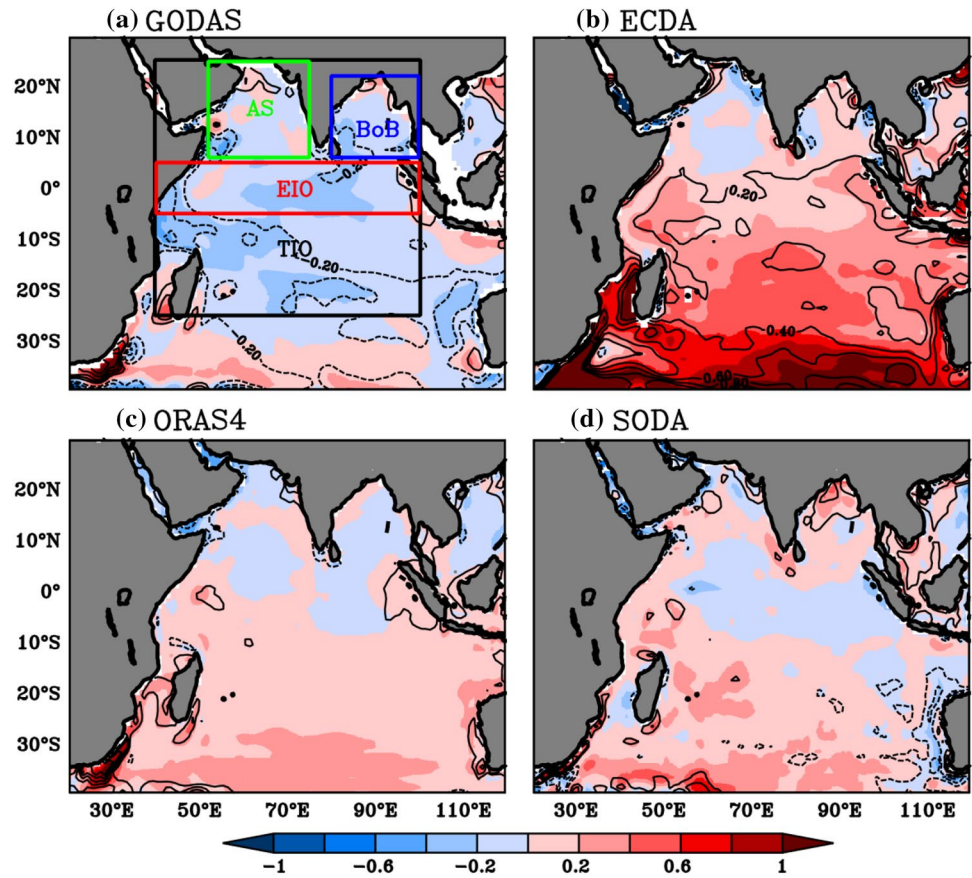

Table 3 Region wise RMSE (pattern correlation) of long term mean fields of SST, SSS, MLD (1980–2010) and zonal and meridional currents (1993–2010) from different reanalyses with respect to HadISST, EN4 analysis and OSCAR currents observations

Region	Reanalysis	SST (°C)	SSS	MLD (m)	U (m/s)	V (m/s)
TIO	GODAS	0.24 (0.99)	0.34 (0.93)	14.78 (0.72)	0.09 (0.69)	0.06 (0.45)
	ECDA	0.32 (0.98)	0.33 (0.94)	12.43 (0.77)	0.09 (0.62)	0.05 (0.52)
	ORAS4	0.12 (0.99)	0.20 (0.98)	13.11 (0.75)	0.07 (0.80)	0.06 (0.44)
	SODA	0.13 (0.99)	0.31 (0.97)	9.29 (0.71)	0.08 (0.75)	0.07 (0.49)
EIO	GODAS	0.15 (0.98)	0.16 (0.99)	12.19 (0.62)	0.15 (0.10)	0.08 (0.14)
	ECDA	0.27 (0.98)	0.18 (0.98)	9.21 (0.66)	0.15 (-0.13)	0.07 (0.26)
	ORAS4	0.14 (0.99)	0.16 (0.99)	7.01 (0.74)	0.11 (0.29)	0.08 (0.20)
	SODA	0.09 (0.99)	0.17 (0.99)	3.97 (0.75)	0.14 (0.18)	0.08 (0.32)
AS	GODAS	0.18 (0.97)	0.17 (0.94)	15.72 (0.76)	0.04 (0.60)	0.03 (0.59)
	ECDA	0.20 (0.97)	0.74 (0.24)	10.64 (0.77)	0.04 (0.53)	0.03 (0.65)
	ORAS4	0.12 (0.99)	0.22 (0.92)	13.09 (0.79)	0.04 (0.54)	0.04 (0.49)
	SODA	0.15 (0.98)	0.23 (0.91)	7.51 (0.56)	0.05 (0.64)	0.05 (0.42)
BoB	GODAS	0.16 (0.83)	0.88 (0.68)	15.19 (0.34)	0.04 (0.62)	0.04 (0.35)
	ECDA	0.22 (0.68)	0.39 (0.91)	10.37 (0.76)	0.05 (0.32)	0.05 (0.29)
	ORAS4	0.09 (0.96)	0.46 (0.90)	9.35 (0.66)	0.05 (0.52)	0.06 (0.08)
	SODA	0.20 (0.87)	0.77 (0.83)	7.02 (0.58)	0.05 (0.60)	0.06 (-0.15)

scores based on concurrent observations of SST, SSS and MLD from RAMA buoy observations from the EIO and BoB (Table 6). The MLD is computed using the potential density criterion based on potential density variations determined from the corresponding 0.125 kg/m^3 (Toyoda et al. 2015).

Table 4 Region wise RMSE (correlation coefficient) of SST, SSS, MLD and currents from different reanalyses with respect to concurrent EN4 analysis and OSCAR currents (35 m averaged) data for respective available period

Region	Reanalysis	SST (°C)	SSS	MLD (m)	U (m/s)	V (m/s)
TIO	GODAS	0.53 (0.85)	0.09 (0.41)	6.76 (0.72)	0.03 (0.70)	0.02 (0.93)
	ECDA	0.28 (0.93)	0.17 (0.31)	14.01 (0.80)	0.03 (0.76)	0.01 (0.94)
	ORAS4	0.36 (0.92)	0.07 (0.77)	14.00 (0.82)	0.02 (0.95)	0.01 (0.96)
	SODA	0.34 (0.93)	0.15 (0.61)	9.24 (0.82)	0.03 (0.77)	0.01 (0.94)
EIO	GODAS	0.46 (0.83)	0.15 (0.27)	6.76 (0.62)	0.14 (0.66)	0.02 (0.85)
	ECDA	0.30 (0.89)	0.22 (0.26)	10.37 (0.71)	0.12 (0.78)	0.02 (0.83)
	ORAS4	0.32 (0.88)	0.18 (0.64)	8.40 (0.73)	0.04 (0.96)	0.02 (0.88)
	SODA	0.37 (0.87)	0.23 (0.43)	6.04 (0.69)	0.11 (0.79)	0.02 (0.84)
AS	GODAS	0.68 (0.82)	0.14 (0.32)	11.12 (0.66)	0.02 (0.93)	0.03 (0.93)
	ECDA	0.45 (0.93)	0.34 (0.04)	13.88 (0.77)	0.02 (0.97)	0.01 (0.97)
	ORAS4	0.44 (0.94)	0.13 (0.60)	16.34 (0.79)	0.02 (0.98)	0.01 (0.99)
	SODA	0.43 (0.93)	0.14 (0.57)	9.22 (0.75)	0.01 (0.97)	0.02 (0.96)
BoB	GODAS	0.49 (0.86)	1.01 (0.14)	10.30 (0.22)	0.03 (0.89)	0.03 (0.48)
	ECDA	0.36 (0.93)	0.35 (0.54)	13.01 (0.38)	0.02 (0.94)	0.03 (0.52)
	ORAS4	0.36 (0.92)	0.34 (0.53)	11.53 (0.52)	0.03 (0.97)	0.02 (0.55)
	SODA	0.32 (0.92)	0.23 (0.73)	7.76 (0.51)	0.03 (0.95)	0.03 (0.42)

Table 5 Region wise standard deviation of SST, SSS, MLD and currents from EN4 analysis/OSCAR data and reanalyses

Region	Data	SST (°C)	SSS	MLD (m)	Data	U (m/s)	V (m/s)
TIO	EN4	0.67	0.08	5.55	OSCAR	0.04	0.02
	GODAS	0.77	0.07	8.62	GODAS	0.04	0.02
	ECDA	0.72	0.14	10.19	ECDA	0.03	0.02
	ORAS4	0.73	0.10	10.76	ORAS4	0.03	0.02
	SODA	0.68	0.15	8.90	SODA	0.03	0.02
EIO	EN4	0.65	0.12	7.37	OSCAR	0.14	0.02
	GODAS	0.60	0.10	8.39	GODAS	0.18	0.03
	ECDA	0.58	0.19	7.28	ECDA	0.15	0.03
	ORAS4	0.59	0.18	8.40	ORAS4	0.14	0.04
	SODA	0.53	0.21	6.26	SODA	0.16	0.02
AS	EN4	1.06	0.14	8.63	OSCAR	0.06	0.04
	GODAS	1.05	0.06	13.75	GODAS	0.05	0.05
	ECDA	1.09	0.22	13.06	ECDA	0.05	0.05
	ORAS4	1.05	0.09	14.90	ORAS4	0.04	0.04
	SODA	0.97	0.15	10.93	SODA	0.06	0.05
BoB	EN4	0.80	0.36	4.69	OSCAR	0.06	0.02
	GODAS	0.93	0.48	9.13	GODAS	0.05	0.03
	ECDA	0.98	0.24	7.44	ECDA	0.04	0.03
	ORAS4	0.89	0.24	7.78	ORAS4	0.03	0.02
	SODA	0.73	0.41	6.03	SODA	0.04	0.02

5 Biases/differences in physical variable of the TIO

5.1 Surface temperature biases and salinity differences

Long term mean SST bias of various reanalyses products with respect to the Reynolds and HadISST are displayed in Fig. 1. GODAS displays mostly negative bias in SST (Fig. 1a), however rest of the reanalyses display positive

bias. The positive bias in ECDA is higher compared to other reanalyses (Fig. 1b). In the case of ORAS4 (Fig. 1c) positive bias is mostly reported south of the equator, with high magnitudes over the south west and west of Madagascar. SODA displays positive bias in the south of 10°S of TIO, north BoB and south of India (Fig. 1d). RMSE in the mean fields of SST is about 0.25 °C (Table 3) with the spatial pattern correlation of 0.99. Error is smaller in ORAS4 followed by SODA, GODAS and ECDA. It is important to

Table 6 RMSE (correlation coefficient) for SST, SSS and MLD of reanalyses data with respect to RAMA buoy observations for EIO and BoB
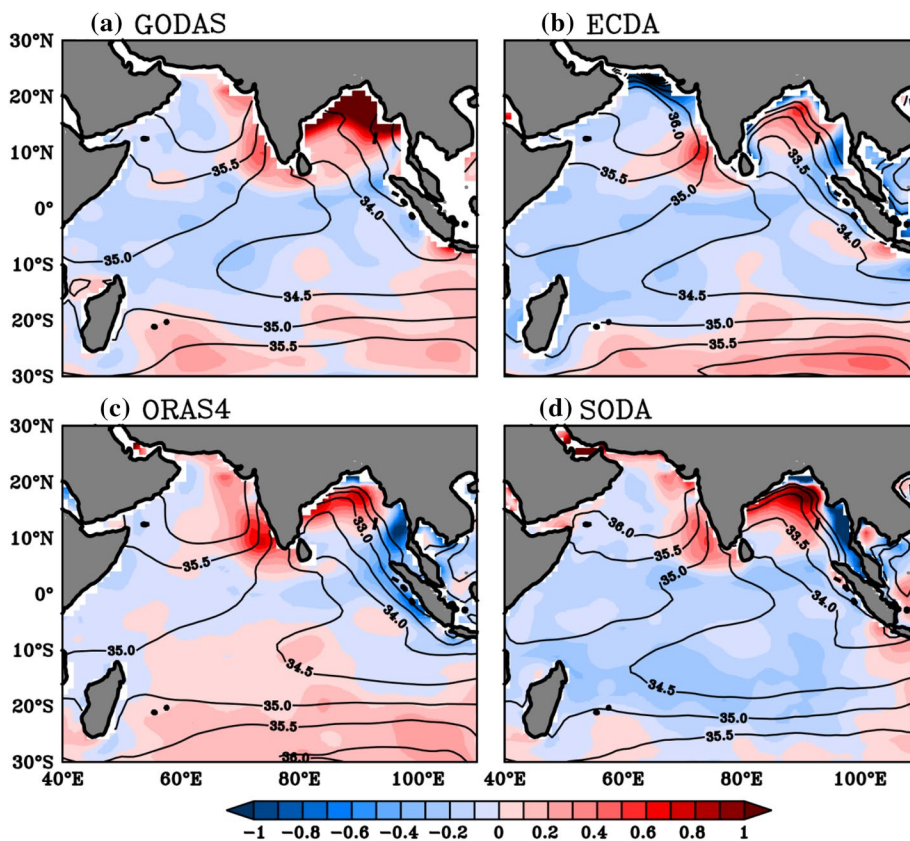
Region	Reanalysis	SST (°C)	SSS	MLD (m)
EIO	GODAS	0.27 (0.92)	0.38 (0.68)	14.02 (0.56)
	ECDA	0.19 (0.94)	0.17 (0.95)	16.59 (0.61)
	ORAS4	0.10 (0.98)	0.14 (0.97)	13.57 (0.77)
	SODA	0.23 (0.92)	0.28 (0.86)	13.00 (0.42)
BoB	GODAS	0.36 (0.92)	0.63 (0.53)	17.71 (0.41)
	ECDA	0.28 (0.95)	0.35 (0.85)	17.14 (0.68)
	ORAS4	0.21 (0.98)	0.34 (0.87)	16.59 (0.69)
	SODA	0.30 (0.95)	0.65 (0.54)	16.78 (0.50)

note that ECDA reanalysis is based on coupled modeling system which does not have any SST restoration; however in other reanalyses SST is restored to observations or climatology (Table 1). The root mean square difference in the climatological SST from Reynolds and HadISST is 0.13 °C over the TIO.

SSS over the TIO has unique characteristics, the AS (BoB) exhibits positive (negative) meridional gradient of salinity. Northern AS and BoB have difference of 4–5 in SSS; this makes them very distinct basins. Apart from this SSS displays 2–2.5 zonal gradient in the EIO. Hence it is

important to simulate the spatial distribution of the TIO SSS by the ocean reanalyses. Most of the reanalyses capture equatorial zonal gradient of salinity well, however all reanalyses underestimated meridional gradient in the BoB. GODAS (Fig. 2a) displays strong positive SSS difference (more than 1) with reference to EN4 analysis in most of the BoB and weak positive difference is reported over the west coast of India and south of 15°S. ECDA shows strong negative difference in the northern AS and along the west coast of BoB and strong positive difference in the north and central BoB, south eastern Indian Ocean and south eastern AS (Fig. 2b). ORAS4 displays mostly positive difference (Fig. 2c), which is higher in the north BoB and south eastern AS compared to other regions. However negative difference is seen in the eastern BoB. SODA shows strong positive salinity difference in the central BoB, whereas it displays negative difference along the eastern coast of BoB (Fig. 2d). This analysis deduces that all the reanalyses have large differences in the BoB and southeastern AS, though these reanalyses are based on different ocean models as well as different data assimilation methodology. RMSE analysis for the mean SSS field over the TIO reveals that ORAS4 displays RMSE of about 0.2 and pattern correlation of 0.93–0.98 (Table 3), however the RMSE is 0.3 in the other reanalyses. Region wise RMSE analysis of SSS indicates that all the reanalyses are more consistent with the EN4 analysis over the

Fig. 2 SSS (at 5 m) differenceswith respect to EN4 analysis over the Indian Ocean from **a** GODAS **b** ECDA, **c** ORAS4 and **d** SODA, contour displays mean surface salinity

EIO and the error is below 0.2, however wide spread of error is reported for the BoB (0.4 and 0.9). This may lead to the underestimation of the upper ocean halocline, responsible for the strongest stratification in the BoB. Root mean square difference between EN4 analysis and WOA climatological salinity fields is 0.09 for the TIO, which is considered as an uncertainty estimate.

5.2 Mixed layer depth differences

MLD represents upper ocean homogeneous layer, which interacts with the atmosphere above and exchanges moisture and heat fluxes. Accurate MLD representation is essential for the proper simulation of ocean state. In general, all the reanalyses display mostly positive MLD differences with respect to EN4 analysis. GODAS shows deeper MLD by 20 m over the northern BoB and south eastern TIO and the region south of India (Fig. 3a). In case of ECDA (Fig. 3b) MLD difference is less than that of GODAS, the north BoB MLD difference is about half of GODAS. Negative MLD difference in the north AS coincides with the unrealistically strong freshening as compared to EN4 (Fig. 2b). ORAS4 shows (Fig. 3c) positive differences in the south Indian Ocean, central BoB and along the west coast of India. However weak negative difference is reported near the equator.

SODA (Fig. 3d) MLD difference is relatively smaller than the other reanalyses and is positive in the north BoB and south of 20°S. SODA displays lowest difference in MLD over the TIO among all the ocean reanalyses, though it is produced by simple data assimilation method (Carton and Giese 2008). MLD RMSE (Table 3) over the TIO range between 10 and 15 m with the correlation of 0.71–0.77 which further support that SODA reanalysis displayed minimum RMSE. Uncertainty estimate based on the root mean square difference between EN4 analysis and WOA climatological MLD fields is 5 m. Overall, in most of the reanalyses positive (negative) MLD difference locations coincide with the positive (negative) salinity difference locations. So misrepresentation of salinity is the prime reason for MLD differences. Region wise MLD RMSE analysis reveals that it is smaller over the EIO compared to the AS and BoB in all the reanalyses, which is consistent with the salinity RMSE in these regions.

5.3 Upper ocean horizontal current biases

Unlike the other tropical oceans, the Indian Ocean currents are eastward over the equator. These current systems are widely known for their role in the transport of heat and salt flux. GODAS shows (Fig. 4a) positive zonal current bias in

Fig. 3 MLD (m) differences with respect to EN4 analysis over the Indian Ocean from **a** GODAS **b** ECDA, **c** ORAS4 and **d** SODA, contour displays mean MLD (m)
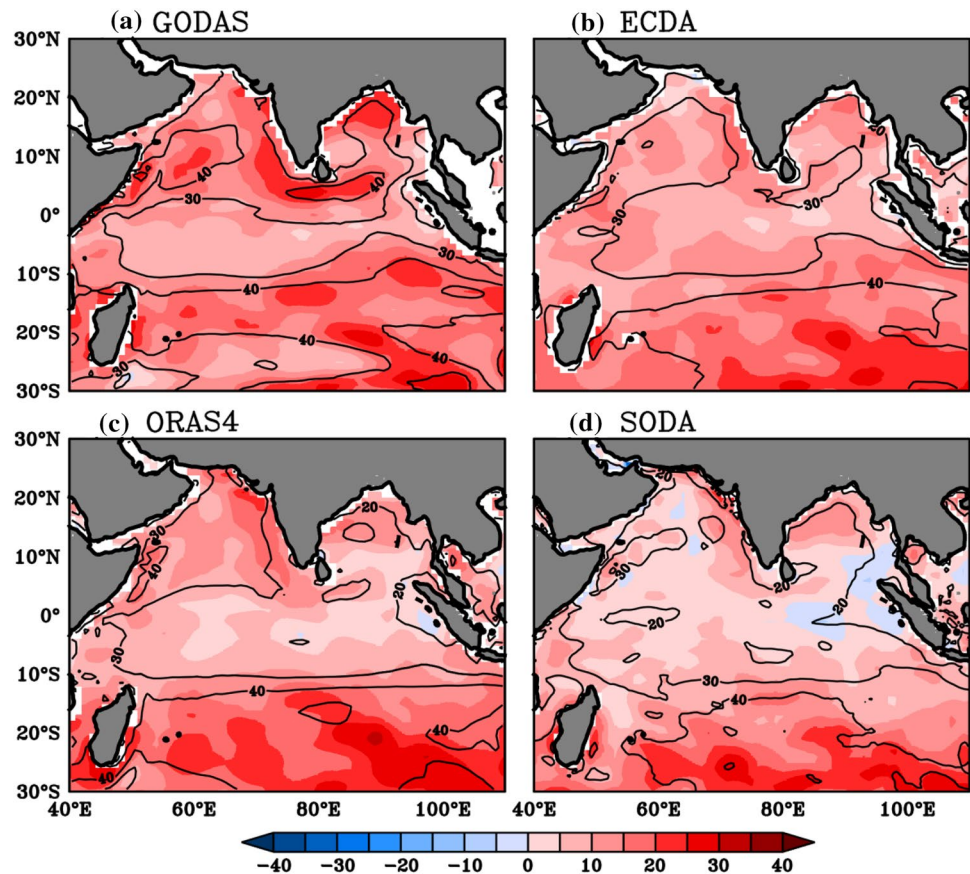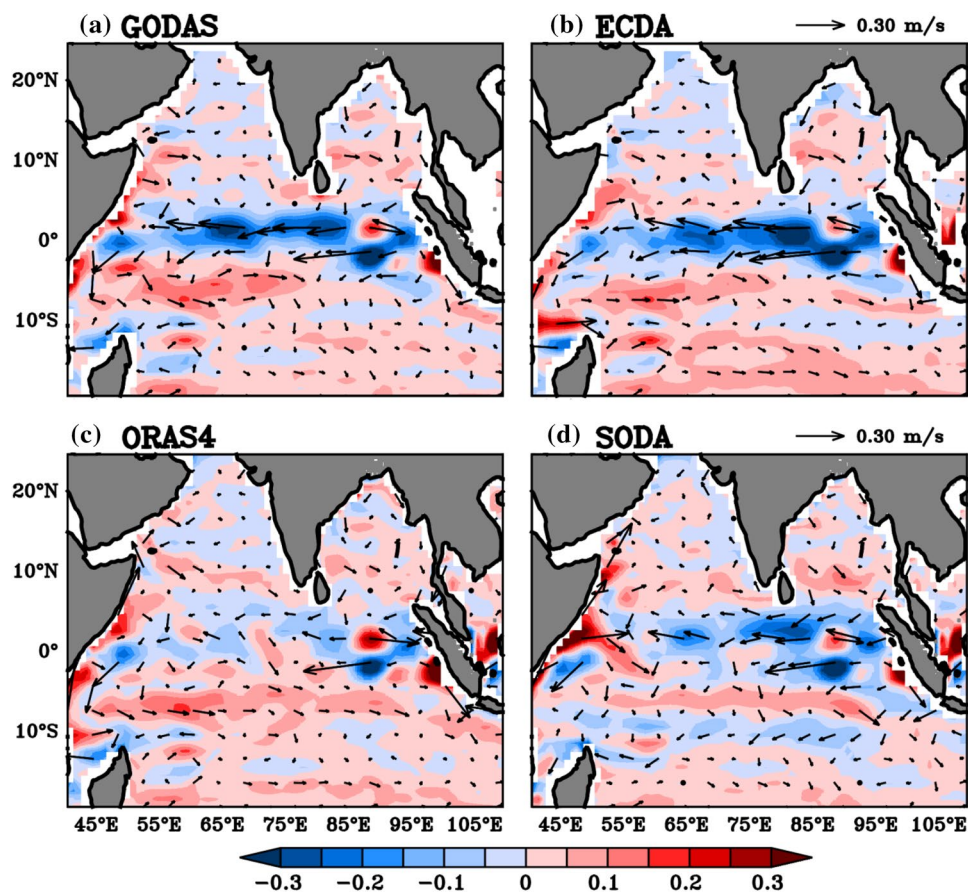
Fig. 4 Current bias (1993–2010, shaded is a zonal current bias m/s) with respect to OSCAR surface current (averaged over upper 35 m) over the Indian Ocean from **a** GODAS **b** ECDA, **c** ORAS4 and **d** SODA
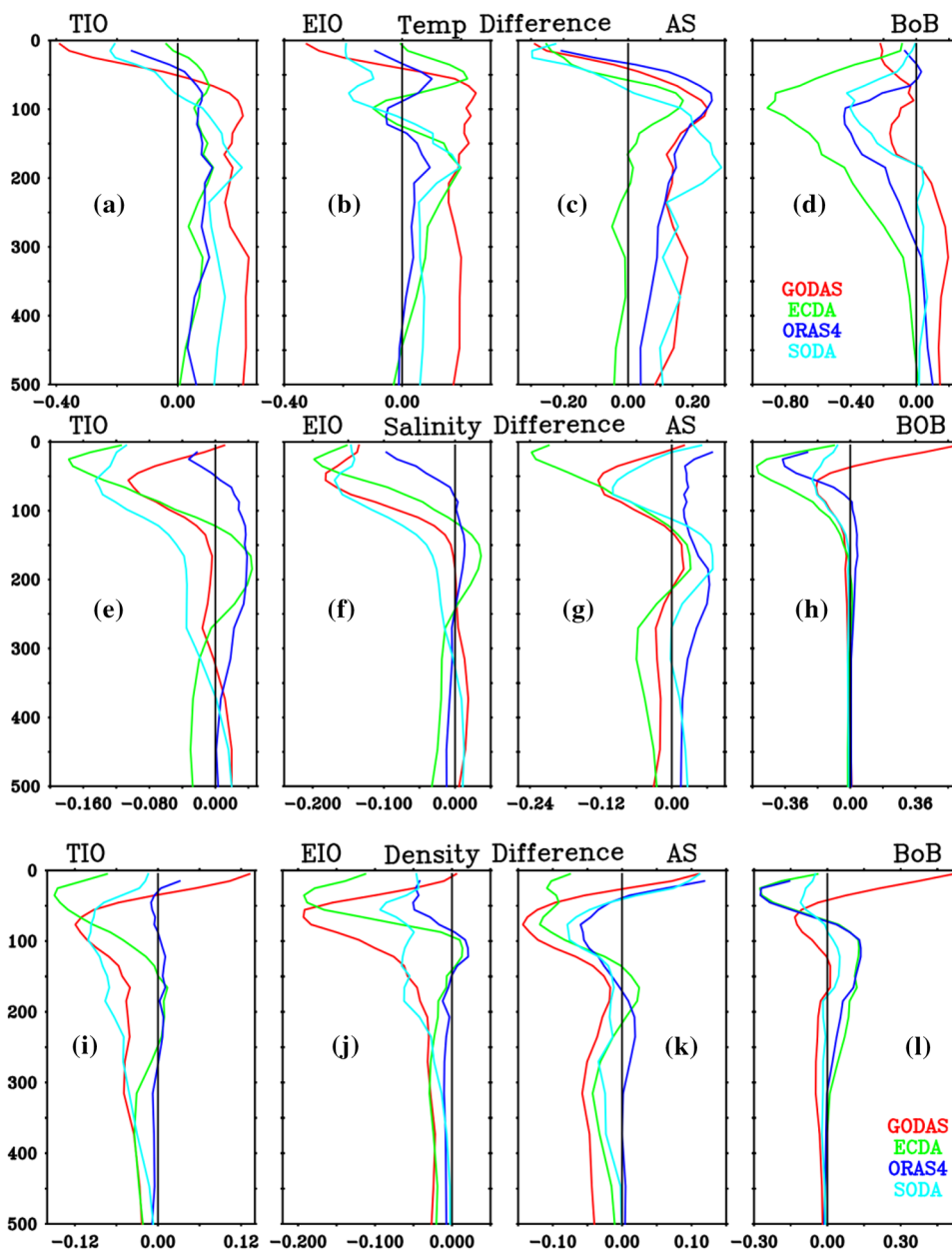

the BoB, southern Indian Ocean and along the Somali coast. Negative zonal current bias is reported over the equator for all the reanalyses. Meridional current displays (figure not shown) southward bias along the Somali coast and south of 10°S. In general meridional current biases are weaker than the zonal current. ECDA shows (Fig. 4b) stronger westward bias in the central and eastern EIO (55°E–90°E). On the other hand eastward bias in the zonal current is dominant south of the equator. GODAS and ECDA current biases over the Indian Ocean have large similarity. ORAS4 shows (Fig. 4c) eastward bias in most of the basin, strongest eastward bias is reported along 8°S. SODA shows (Fig. 4d) westward current bias at the equator and 10°S, with eastward bias in the rest of the basin. Overall GODAS, ECDA and SODA display westward bias at the equator indicating weaker Wyrtki jet and associated counter currents. ORAS4 shows weaker biases than the rest of the reanalyses. Nyadjro and McPhaden (2014) reported that horizontal currents from ORAS4 reproduce the variability of currents in the EIO associated with the IOD reasonably well. Region wise RMSE analysis of horizontal current (Table 3) reveals that over the AS and BoB current displays less RMSE than EIO. Among all reanalyses ORAS4 and SODA display lowest RMSE (and higher pattern correlation) in zonal current followed by GODAS and ECDA. Balmaseda et al. (2013)

found that assimilation of actual T and S profiles with sea level anomaly from altimeter improves the sea level representation in the tropical regions which resulted better circulation in ORAS4. Over the EIO zonal currents in all the reanalyses display pattern correlation less than 0.3 indicating that reanalyses could not capture the pattern of zonal current properly in the EIO. This is equally true for the EIO and BoB meridional currents.

5.4 Vertical structure of differences

Above discussion is mostly confined to the upper ocean; however it is equally important to study the structure of mean vertical profile of physical variables. Error in the vertical profiles of physical variables can produce strong differences in temperature at the surface and subsurface which may lead to improper simulation of mean (Chowdary et al. 2016) and variability. This section explores the nature of temperature, salinity and density differences with depth over the TIO and in particular over the AS, BoB and EIO with respect to EN4 analysis (Fig. 5). Over the TIO (Fig. 5a), GODAS shows highest negative temperature difference in the top 50 m; however all the reanalyses displays positive difference below 100 m. ORAS4, SODA and ECDA display almost similar vertical pattern of temperature difference.

Fig. 5 Vertical profile **a–d** temperature difference (°C), **e–h** salinity difference, **i–l** Density difference (kg/m³) with respect to EN4 analysis, for TIO, EIO, AS and BoB from GODAS, ECDA, ORAS4 and SODA

Region wise analysis reveals that the BoB displays (Fig. 5d) diverse pattern of difference compared to the EIO and AS (Fig. 5b–c). ECDA displays strong negative difference (− 1 °C) in the BoB at 100 m, however most of the reanalyses display positive difference in the AS subsurface, with maximum difference at 50 m (0.35 °C). Uncertainty in vertical temperature field is 0.13 °C over the TIO. In the case of salinity (Fig. 5e–h), ECDA and SODA show negative salinity difference in the upper ocean however GODAS displays weak positive salinity difference over the TIO (Fig. 5e). Over the EIO (Fig. 5f) all the reanalyses show negative difference in the first 150 m (it is 50 m in ORAS4). Hence most of the reanalyses underestimate salinity in the upper 150 m of the EIO. Over the AS (Fig. 5g) ORAS4, SODA and

GODAS show small positive difference at surface, ECDA on the other hand shows negative difference with maximum negative difference at about 25 m. ORAS4 displays positive difference throughout the water column. Uncertainty in the vertical salinity field is 0.035 over the TIO. In the case of BoB (Fig. 5h) GODAS shows positive difference at the surface; however the rest of the reanalyses display negative differences. ECDA and ORAS4 show maximum negative difference (0.5) in the subsurface (about 50 m).This strong negative difference in subsurface specifies more freshwater than EN4 analysis. Fousiya et al. (2015) reported that in GODAS excess mixing due to weaker stratification supports deeper extent of freshwater. Above discussed temperature and salinity differences contribute to density leading to

difference in the upper ocean stability. All the reanalyses (except GODAS) display negative density difference over the TIO (Fig. 5i), however ORAS4 displays very little density difference. Strongest negative difference is reported by ECDA in the TIO as well as in all regions. In the BoB GODAS displays strong positive (negative) density difference in upper (below) 50 m (Fig. 5l), however all the other reanalyses display negative difference in the upper 100 m. In general vertical structure of density difference corroborates with the salinity difference structure in all the reanalyses.

Since actual observations/analysis of horizontal currents profile is not available, mean currents profile from different reanalyses are inter-compared for the period of 1993–2010. Vertical structure of zonal current over the TIO displays noticeable discrepancy among reanalyses products in the upper 100 m (Fig. 6a–d). All the reanalyses display westward current in the TIO upper ocean. However over the EIO (Fig. 6b) mean currents are eastward due to dominant Wyrtki Jets (Wyrtki 1973). In the case of AS (Fig. 6c) top 100 m displays eastward current (associated with the strong south west monsoon forcing) and it is westward between 100 and 300 m. Surface current is also eastward in the BoB (Fig. 6d), and subsurface (between 100 and 300 m) current is westward. Overall these reanalyses are able to capture TIO current features more consistently. The vertical structure of zonal current of GODAS in the AS does not seem much more pronounced than the other reanalyses, however

in the BoB it (Fig. 6d) differs from the other reanalyses and displays strong vertical shear in the upper ocean compared to other reanalyses. Meridional currents (Fig. 6e–h) over the TIO display smaller discrepancy compared to zonal currents. All the reanalyses display surface currents southward in the first 75 m and northward below it. The strength of upper ocean current is higher in the GODAS compared to rest of the reanalyses. In the EIO (Fig. 6f) southward current is highest at 50 m and northward at 100 m, relatively better inter consistency is reported among different ocean reanalyses. This structure of current represents meridional overturning circulation cell (Schott et al. 2002), where upper ocean currents are pole ward and deeper ocean currents are equator ward. Over the AS (Fig. 6g) GODAS displays southward surface currents; however rest of the reanalyses display northward surface currents. In the BoB (Fig. 6h) GODAS displays strong southward current compared to rest of the reanalyses in the upper ocean. GODAS current at 80 m is northward though current is southward in other reanalyses. This indicates that all the reanalyses products display good consistency in the AS and BoB except GODAS.

5.5 Upper ocean processes associated with differences

To understand the role of vertical stability and shear instability processes to upper ocean differences, square of the Brunt–Vaisala frequency (BV) with respect to EN4 analysis

Fig. 6 Vertical profile, **a–d** zonal current (m/s) and **e–h** meridional current (m/s) for TIO, EIO, AS and BoB from GODAS, ECDA, ORAS4 and SODA

and vertical shear of horizontal currents are studied in each reanalyses. Figure 7(a–d) displays the BV difference, all the reanalyses show negative difference of the BV in the upper ocean over the TIO, highest negative difference is reported by GODAS at 25 m. In the EIO similar nature of the BV difference is reported (Fig. 7b). In the case of AS, the BV difference is relatively higher than the EIO in upper ocean and most of the reanalyses are consistent with each other for the AS and EIO except ECDA, which shows positive difference at 20 m (Fig. 7c). In the BoB vertical gradient of density is larger than any other basin in the TIO (e.g., Agarwal et al. 2012). In other words the BV is high in the BoB, all reanalyses show that the BV difference over the BoB is more than double compared to the rest of the basins. The negative difference in the BV at surface clearly indicates that all the reanalyses underestimate stability of the BoB for the upper 30–40 m (70 m in GODAS). Overall upper ocean stability is weaker in GODAS in all the basins, compared to the other reanalyses. Figure 7(e–h) displays the nature of vertical shear of horizontal current from different reanalyses. In the TIO (Fig. 7e) except ORAS4, other reanalyses show decreasing shears with depth and very sharp gradient in the upper ocean. GODAS and ECDA display similar profiles of shear, however SODA shows highest shear in the upper 20 m. In the EIO (Fig. 7f), large discrepancy is noted in the shear profiles of currents from different reanalyses compared

to other regions of the TIO. In the AS and BoB (Fig. 7g, h) shear profiles are similar to that of the TIO. SODA shows higher shear in the upper 20 m followed by ECDA, GODAS and ORAS4. SODA and ECDA overestimate current shear with respect to GODAS. Fousiya et al. (2015) reported that in the BoB upper ocean horizontal current shear is over estimated by GODAS with respect to in-situ buoy observations. Above analysis supports that upper ocean stratification/stability is underestimated by the reanalyses products and mostly shear is overestimated supporting the positive bias of MLD and SSS. Further contribution of salinity and temperature differences to density differences are studied.

According to the equation of state, differences in temperature and salinity affect the density difference. Contribution of temperature and salinity difference to density difference is estimated using Eq. (3). Figure 8(a–d) displays contribution of temperature difference to the density difference, where temperature difference is with respect to EN4. GODAS, ORAS4 and SODA show (Fig. 8a) negative difference in the upper ocean, however below 50 m they show positive difference in the TIO. Below 100 m all the reanalyses show small positive contribution of temperature difference to density difference. Over the EIO and AS (Fig. 8b), reanalyses show similar nature of contribution to density difference throughout the upper 500 m. In the BoB (Fig. 8d) notable negative density difference due to temperature difference is

Fig. 7 Vertical profiles of **a–d** square of Brunt–Vaisala frequency difference with respect to EN4 analysis (s^{-2}) and **e–h** vertical shear of horizontal currents (s^{-2}) from GODAS, ECDA, ORAS4 and SODA over the regions TIO, EIO, AS and BoB, respectively
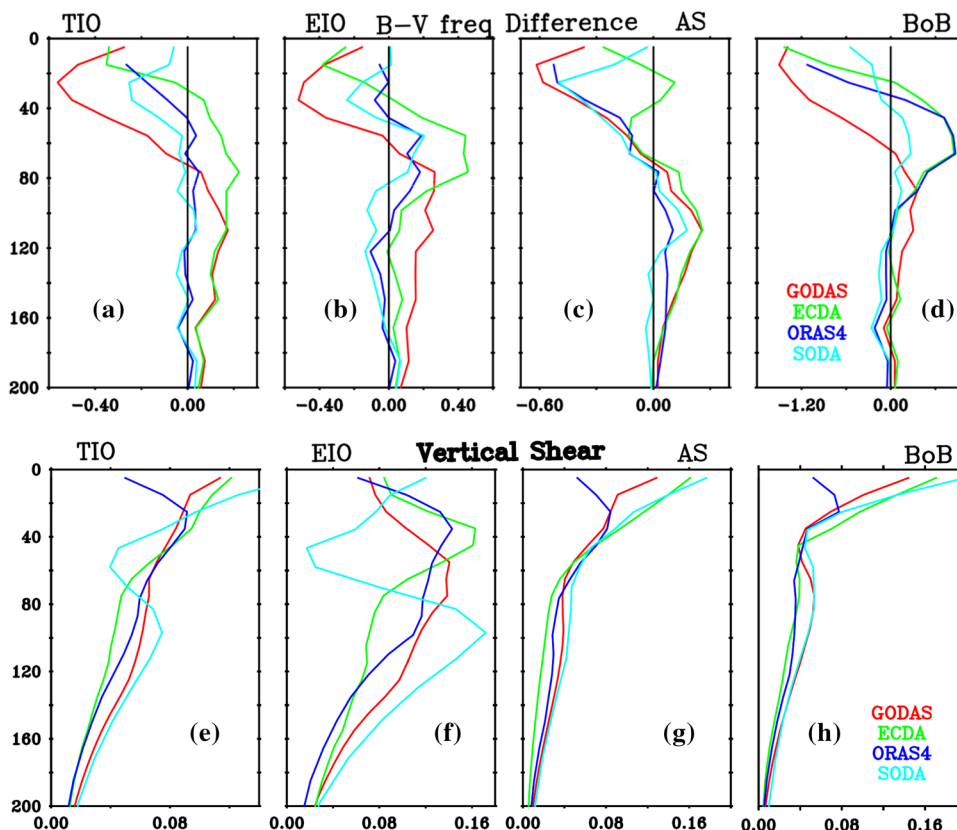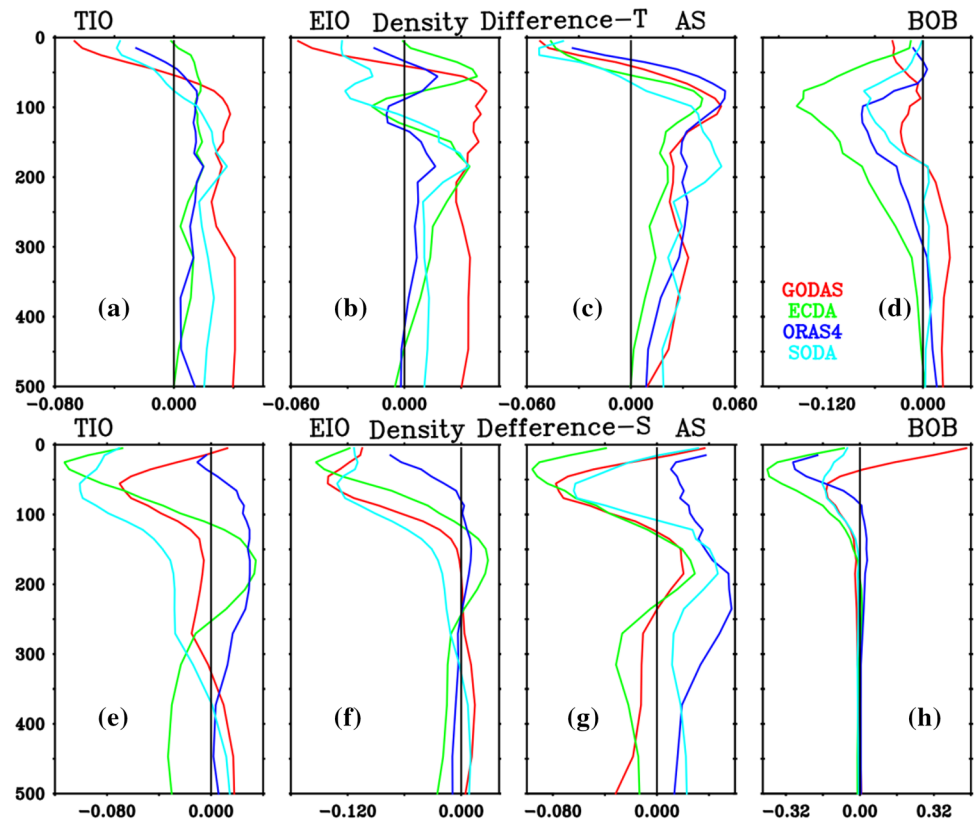
Fig. 8 Vertical profile of **a–d** contribution of temperature difference to the density difference and **e–h** salinity difference to density difference from GODAS, ECDA, ORAS4 and SODA over the regions TIO, EIO, AS and BoB, respectively. Here temperature and salinity differences are with respect to the EN4
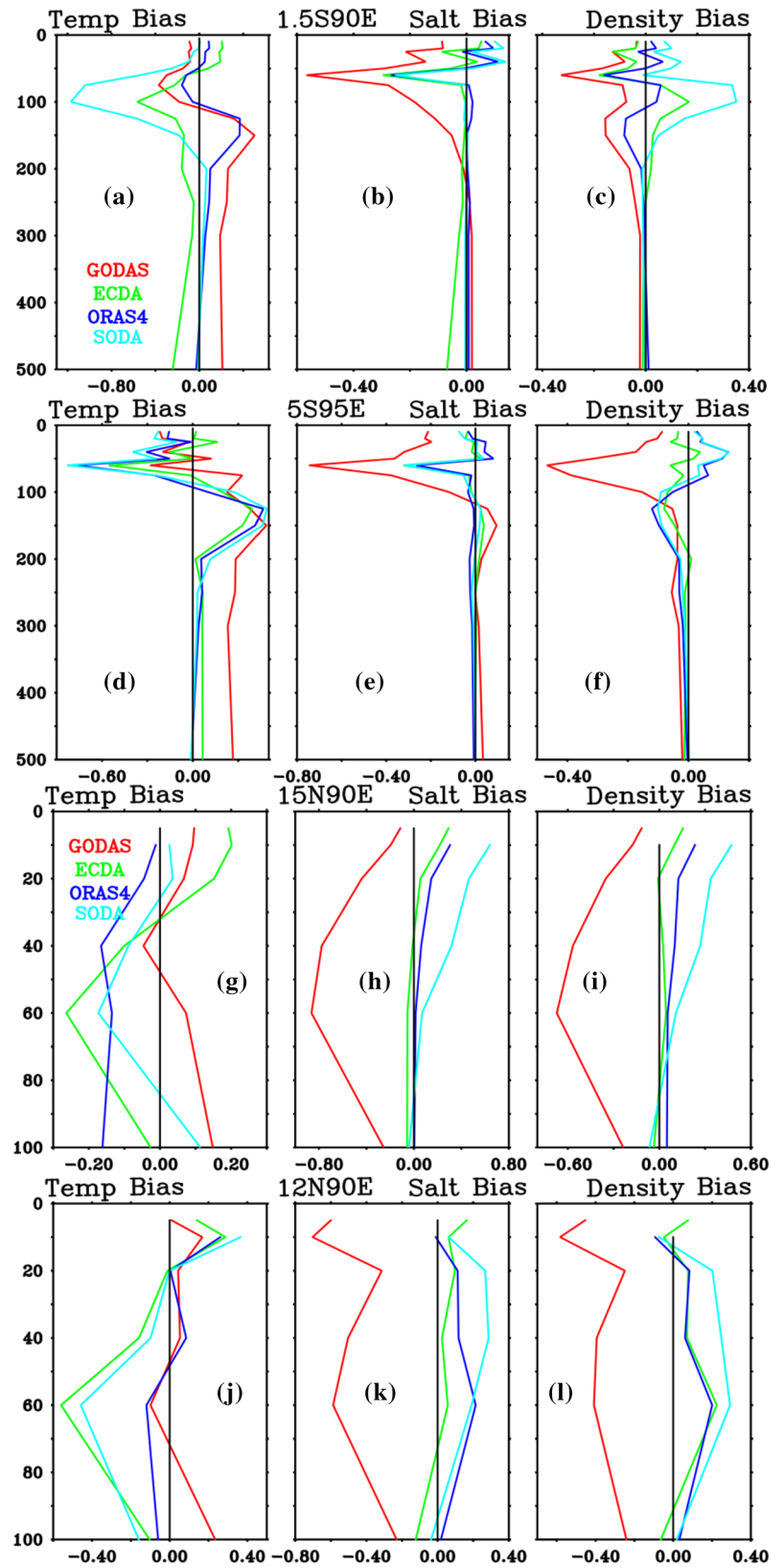

found throughout the column. ECDA displays higher magnitudes compared to the rest of the reanalyses. Overall the contribution of temperature difference to density difference is maximum in the BoB. Figure 8(e–h) displays contribution of salinity difference to the density difference, where salinity difference is with respect to EN4. In the case of TIO (Fig. 8e) ECDA and SODA display negative density difference in the upper ocean, however GODAS displays weak positive difference. Highest negative difference is reported at about 20 m in the ECDA. In the EIO (Fig. 8f) salinity difference contributed negatively to density difference in the upper 100–200 m in all the reanalyses. GODAS, ECDA and SODA are consistent with each other; however ORAS4 displays smaller contribution to density difference. Similar consistency is reported in the AS also (Fig. 8g), ORAS4 shows positive contribution of salt difference in density difference throughout the upper ocean. In the case of BoB (Fig. 8h) GODAS shows positive contribution to density difference due to salinity difference in the upper 50 m however the rest of the reanalyses display negative difference in the upper Ocean. Compared to rest of the basin the BoB salinity differences are contributing largely to the density differences. Overall, the contribution of salinity differences to density differences is higher than that of temperature differences. The pattern of profile of salinity difference and density difference are matching with each other (Fig. 5i–l). Above discussion indicates that salinity differences need to

be rectified in these reanalyses products to improve upper ocean density structure, which may in turn help to improve the upper ocean stability and reduce excess mixing, thereby reducing the MLD differences.

5.6 Vertical structure of biases with respect to RAMA buoys observations

Figure 9 displays the vertical profiles of temperature, salinity and density biases with respect to RAMA buoy (here two buoys from the EIO and two buoys from the BoB are displayed which are having largest concurrent observations). In case of temperature (Fig. 9a, d) bias is small in the upper 40 m but noticeable (−1 °C) negative bias is reported between 50 m to 150 m. SODA displays higher biases compared to ECDA, GODAS and ORAS4. In case of salinity (Fig. 9b, e), notable bias is reported between 50 and 100 m depth. Maximum bias of 0.3 is reported at about 50 m in ORAS4, whereas it is about 0.5 in GODAS. In general all the reanalyses underestimate salinity in the 50–100 m and most reanalyses do a good job for 100–500 m. Biases in the upper 100 m lead to the underestimation of density in GODAS (Fig. 9c, f). Which leads to the underestimation of stratification of thermocline in GODAS. Above analysis supports that over the EIO strong biases in temperature and salinity exist in the reanalyses at subsurface levels.

Fig. 9 Mean vertical profile of potential temperature (°C), salinity and potential density (kg/m^3) biases from the EIO (**a**–**f**) and BoB RAMA buoys (**g**–**l**)

In case of the BoB (Fig. 9g–l) subsurface observations of temperature and salinity are available up to 100 m only. In case of temperature (Fig. 9g–j) notable biases are found below 40 m. In the upper levels (< 30 m) weak warm bias is found, however mostly cold bias is reported below that in the reanalyses (except GODAS). In the case of salinity (Fig. 9h–k) except GODAS rest of the reanalyses display weak positive bias in the upper 40–60 m, however GODAS displays negative bias throughout the upper 100 m and its magnitude is ranging from 0.4 to 0.8. This supports our hypothesis that GODAS mixes surface fresh water to the deeper depth. This finding resembles that of Fousiya et al. (2015), in which they reported that horizontal current shear is responsible for the excess mixing of fresh water to deeper depth in GODAS for the BoB. These biases in temperature and salinity lead to biases in the density (Fig. 9i, l), negative density bias (> 0.4 kg/m³) is dominating in GODAS throughout the upper ocean, however rest of reanalyses display positive density bias. This underestimation of density in GODAS can lead to underestimation of vertical stratification in the upper ocean of the BoB. This in turn contributes to positive biases in the mixed layer and thermocline in the GODAS. All together this section suggests that reanalyses products display negative subsurface bias in density over the BoB. Among all reanalyses GODAS salinity and density profiles deviate much from the buoy observations of the BoB.

5.7 RMSE evolution in the seasonal climatology

Since the Indian Ocean has strong seasonality and these reanalyses products are widely used for the seasonal forecast, apart from annual mean RMSE analysis it will be equally important to study month wise evolution of RMSE in all the physical variables. In general annual cycle is divided in to four seasons, spring (March–May), summer (June–September), fall (October–November) and winter (December–February). Studies have reported that the coupled model seasonal forecast skill is sensitive to the initial condition (e.g., Chattopadhyay et al. 2015). This enforced us to study month wise RMSE evolution. Figure 10 shows the temporal evolution of mean RMSE in SST, SSS, MLD and zonal currents for the TIO as well as for sub region in different reanalyses. Month wise RMSE evolution of SST (Fig. 10a) does not show any specific dependency on time in ORAS4, ECDA and SODA; however in GODAS higher RMSE during March–June compared to rest of the year is reported. Chattopadhyay et al. (2015) reported that the Indian summer monsoon forecasts using coupled model exhibits better skill with February initial conditions compared to that of April/May initial conditions. Oceanic initial conditions from GODAS, displays larger RMSE during March–June compared to rest of the year. Region wise RMSE evolution

supports that all the regions display higher RMSE during spring in GODAS (Fig. 10a–d).

Figure 10e–h shows the RMSE in SSS, in the TIO (Fig. 10e). RMSEs are less during spring and summer and RMSEs are higher in winter and fall. Region wise RMSE analysis shows that SODA displays higher RMSE in the BoB during fall (Fig. 10h), however ECDA displays higher RMSE in the AS during summer and fall (Fig. 10g), which is also consistent with the salinity biases (Fig. 2b). MLD RMSE evolution (Fig. 10i–l) displays annual cycle which has higher magnitude during spring to summer and lower in fall and winter. The AS displays higher MLD RMSE during spring and summer, whereas the BoB displays during winter. Temporal evolution of RMSE in ORAS4, SODA and ECDA are more consistent with each other, however GODAS displays inconsistency in the temporal evolution as well as higher RMSE magnitude compared to other reanalyses products. In case of zonal currents (Fig. 10m–p) higher RSMEs are in July and August in most of the reanalyses and they are strong over the EIO. Overall ORAS4 shows least RMSE in most of the variable and which remains constant throughout the year.

5.8 Temporal variability and RMSE status in different analysis

5.8.1 RMSE evolution with EN4 analysis

Here each reanalysis is compared with EN4 analysis for each time step (total time steps 372 in case of SST, SSS, and MLD for period of 1980–2010 and 216 time steps in case of zonal and meridional currents for the period 1993–2010 and compared with OSCAR) for the respective region. In this way region wise averaged data sets are generated for each variable for all the reanalysis. Data set consisting of two time series (one from analysis and another from reanalysis) is used to estimate the RMSE. OSCAR monthly observations of zonal and meridional currents averaged over the upper ocean ~ 35 m are considered as upper ocean currents. Table 4 displays RMSE and correlation coefficient for the above discussed parameters over the TIO as well as over the sub regions (EIO, AS and BOB). The mean temperature and salinity at the first level of reanalyses (as well as EN4 analysis at 5 m) are respectively called as SST and SSS. In case of SST, RMSE range for the TIO is about 0.3–0.5 °C in different reanalyses with correlation coefficient ranging from 0.85 to 0.9. This supports that temporal evolution of SST is better captured by all the reanalyses over the TIO. RMSE is minimum in ECDA followed by SODA, ORAS4 and GODAS. Region wise analysis indicates that SST RMSE is in the order of 0.3–0.7 °C and higher RMSE is reported over the AS compared to the BoB and EIO. However correlation is more consistent among the reanalyses
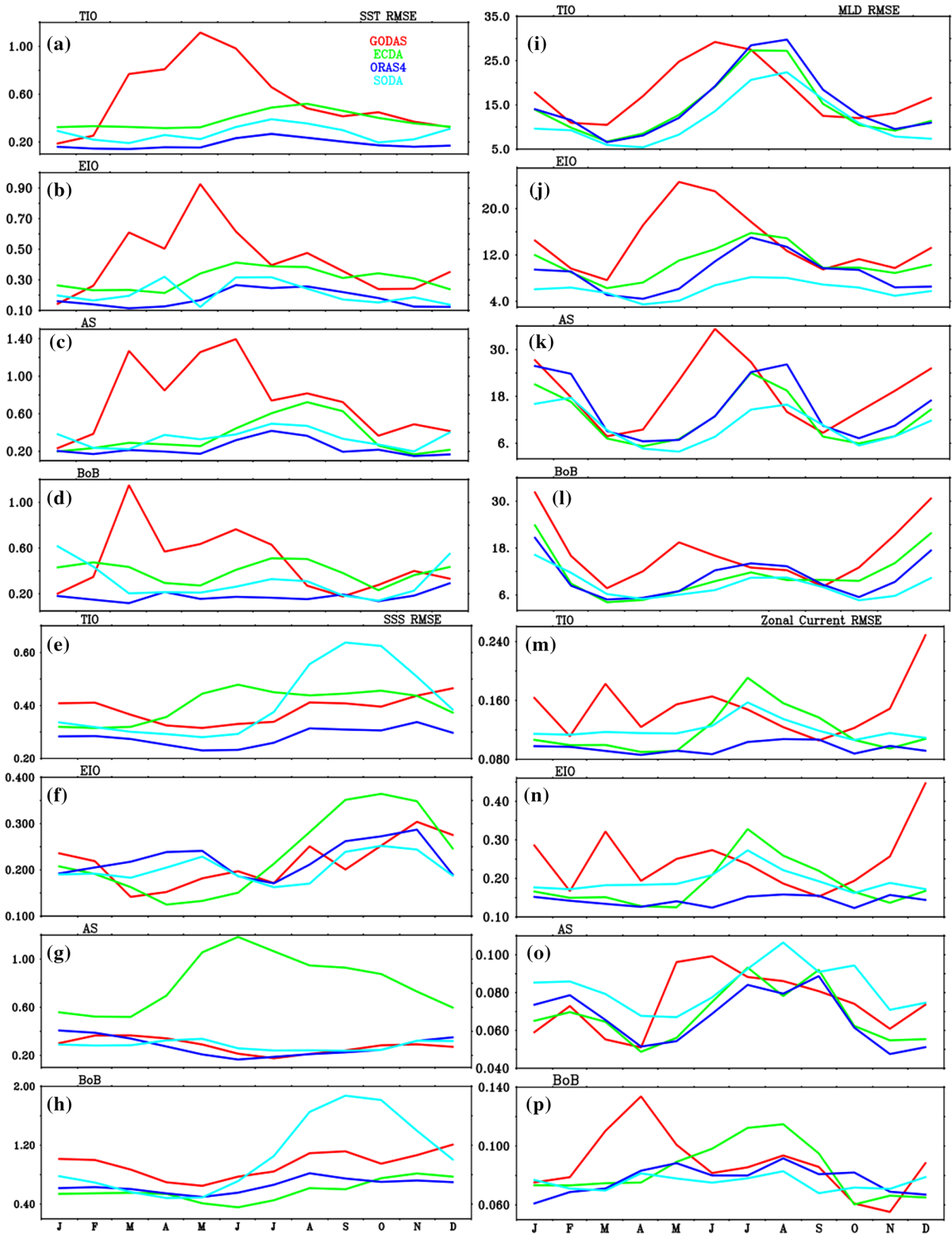
Fig. 10 Monthly evolution of RMSE of **a–d** SST (°C), **e–h** SSS, **i–l** MLD (m) and **m–p** zonal currents (m/s) for the TIO, EIO, AS and BoB, respectively

over all the sub regions. The salinity RMSE over the TIO range between 0.07 and 0.17 and correlation ranges from 0.3 to 0.77. Minimum RMSE and highest correlation is displayed by ORAS4 followed by SODA, GODAS and ECDA. Region wise analysis reveals that lowest RMSE is reported over the AS. Correlation for the BoB salinity is lowest in GODAS. MLD displays RMSE range of 7–14 m over the TIO and the correlation coefficient between 0.7 and 0.8 for the reanalyses. The above analysis supports that reanalyses capture the temporal evolution of MLD in the TIO. Region wise analysis indicates higher errors over the AS and BoB compared to the EIO and the correlation over the BoB is lower than other regions. Hence this supports that temporal evolution of MLD over the AS and EIO are better captured by the reanalyses compared to the BoB. RMSE in zonal current range between 0.02 and 0.03 m/s and correlation is 0.7–0.95. ORAS4 displays minimum error and maximum correlation over the TIO. RMSE (correlation) over the AS and BoB for zonal current is less (high) in all the reanalyses, however over the EIO RMSE is higher mainly in GODAS, ECDA and SODA reanalyses. In the case of meridional currents RMSE is lower than zonal currents and correlation coefficient is higher in all the reanalyses. This supports that all the reanalyses capture meridional currents better. Region wise RMSE analysis indicates that slightly higher RMSE and lower correlation is reported in all the reanalyses for the BoB. ORAS4 displayed lowest error and highest correlation compared to the other reanalyses.

5.8.2 Variability assessment with respect to EN4 analysis

Table 5 displays standard deviation (SD) of SST, SSS and MLD for the period of 1980–2010 from EN4 analysis, GODAS, ECDA, ORAS4 and SODA. The SD score gives strength of the variability of the parameter. In case of SST variability over the TIO is 0.7 °C, which is almost captured by all the reanalyses. The strength of SST variability over the TIO is higher than the RMSE reported in the reanalyses (Table 4). Region wise analysis shows that high SST variability is reported over the AS and BoB, followed by the EIO. All the reanalyses capture this region wise variability of SST. The EN4 analysis displays the salinity variability of 0.08, all the reanalyses except GODAS over estimates the variability strength over the TIO. The strength of variability and RMSE in the reanalyses for salinity (Table 4) is of same order. Region wise analysis indicates that highest variability is reported in the BoB followed by the AS and EIO. Reanalyses products capture this regional pattern of SSS variability. In case of MLD EN4 analysis displays variability by 5 m in the TIO, however reanalyses overestimate it. Region wise analysis indicates that the EIO and AS display higher MLD variability compared to BoB. SODA captures MLD variability better over the AS and BoB however over the

EIO ECDA is better compared to others. Table 5 also displays SD of zonal and meridional circulation for the period of 1993–2010 from OSCAR, GODAS, ECDA, ORAS4 and SODA. In case of zonal circulation reanalyses could capture variability (~0.04 m/s) like in OSCAR over the TIO. Variability and strength of RMSE over the TIO for the horizontal circulation are in same order. OSCAR displays highest variability in zonal circulation in the EIO followed by the BoB and AS, reanalyses could capture this nature of zonal circulation but mostly overestimates variability in the EIO and underestimates in the AS and BoB. In case of meridional currents reanalyses are consistent with OSCAR over the TIO. Region wise analysis indicates that reanalyses mostly overestimate the variability in the AS, EIO and BoB. Overall the ocean reanalyses display variability and RMSE of same order in the case of SSS, MLD, zonal and meridional currents for the TIO as well as for sub regions.

5.8.3 Error evolution from RAMA buoys observations

Figure 11 displays scatter plots for SST (a–d), SSS (e–h) and MLD (i–l) from reanalyses and RAMA buoys over the EIO region. There were ten buoys providing observations during the study period covering the region 80°E–90°E and 4°N–4°S (Table 2). About 500 concurrent samples are obtained. It is important to note that RAMA observed temperature data are converted to potential temperature before error analysis is carried out. Figure 11a–d displays the scatter for SST for different reanalyses. All the reanalyses display warm bias, error for GODAS and SODA is about 0.25 °C and for ECDA and ORAS4 it is 0.2 and 0.1 °C (Table 6) respectively. Scatter analysis of SSS for different reanalyses indicates that all the reanalyses overestimate SSS (Fig. 11e–h). Error in GODAS and SODA is 0.3, in ECDA and ORAS4 is about 0.15. SSS evolution is better simulated by ECDA and ORAS4 followed by SODA and GODAS. It is important to note that the fresh-water flux in ORAS4 is corrected through the global sea-level changes from the altimeter (Balmaseda et al. 2013), which is not the case for other reanalyses. Figure 11i–l displays scatter plots for the MLD, where MLD is estimated following Toyoda et al. (2015) potential density criteria. All the reanalyses overestimate the MLD compared to RAMA. Error over the EIO in SODA, ORAS4 and GODAS is about 13 m however ECDA displays slightly higher MLD (16 m, Table 6). In the case of SODA though the error is 13 m but the correlation is about 0.42, however in other analysis it is greater than 0.6. In general MLD variability over the EIO is about 8 m which is of the order of error reported with respect to RAMA observations. Overall, all reanalyses display higher MLD errors with RAMA observation than RMSE with EN4 analysis over the EIO.
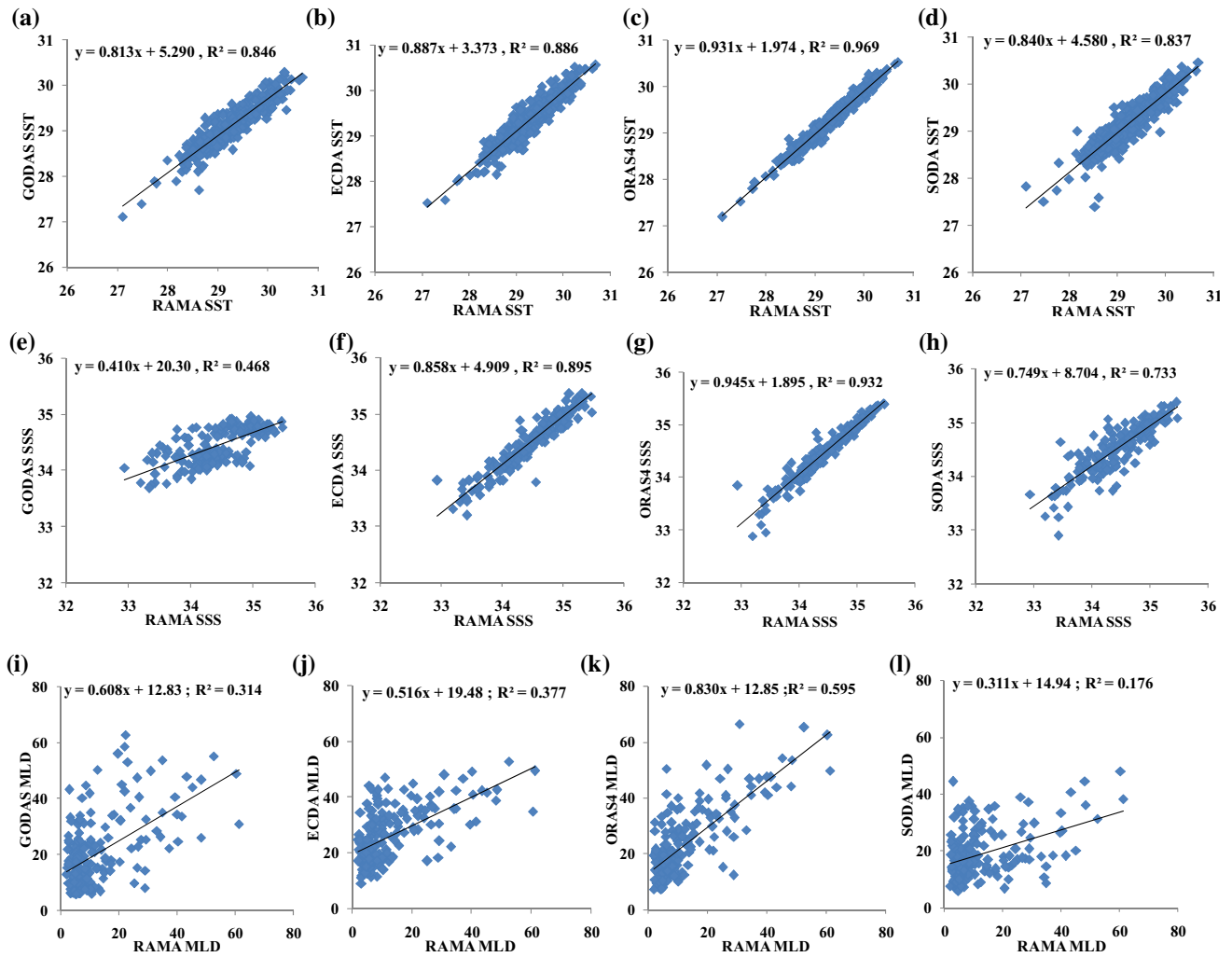
Fig. 11 Scatter plots of RAMA buoys observations against the reanalyses data for **a–d** SST (°C), **e–h** SSS and **i–l** MLD (m) from EIO region

Figure 12 displays scatter plots for SST (a–d), SSS (e–h) and MLD (i–l) from reanalyses and RAMA buoys over the BoB region. There were three buoys providing observation during the study period covering the region 90°E and 8°N–15°N (Table 2). In case of SST (Fig. 12a–d) all the reanalyses display warm bias with high correlation, suggesting temporal evolution of SST in reanalyses is consistent with that of RAMA buoy observations in the BoB. Error estimates (Table 6) for GODAS is 0.36 °C, for ECDA and SODA it is 0.28 °C and for ORAS4 it is 0.21 °C. Figure 12e–h shows the scatter plots for SSS from all the reanalyses and RAMA observed. All the reanalyses display positive bias, supporting overestimation of salinity in the BoB. RAMA (reanalyses) displays a range of SSS from 31 to 34 (32–34). Error in case of GODAS and SODA (ECDA and ORAS4) is 0.6 (0.3, Table 6). These errors in reanalyses product are higher than the variability of SSS over the BoB. Figure 12i–l shows the scatter plots

for MLD, all the reanalyses overestimate MLD and display error about 17 m (Table 6). Hence with actual observations all the reanalyses display errors of almost same order, secondly all the reanalyses display higher error over the BoB compared to other regions. In general ORAS4 and ECDA are performing better over the BoB compared to GODAS and SODA. Further ORAS4 is displaying good consistency between low error and higher correlation coefficient compared to other reanalyses.

6 Summary and conclusion

Present study focuses on the inter-comparison of long term mean of the TIO SST, SSS, MLD, and horizontal currents obtained from widely used reanalyses products (GODAS, ECDA, SODA and ORAS4) with respect to observations as well as the base line data (i.e., EN4 analysis).
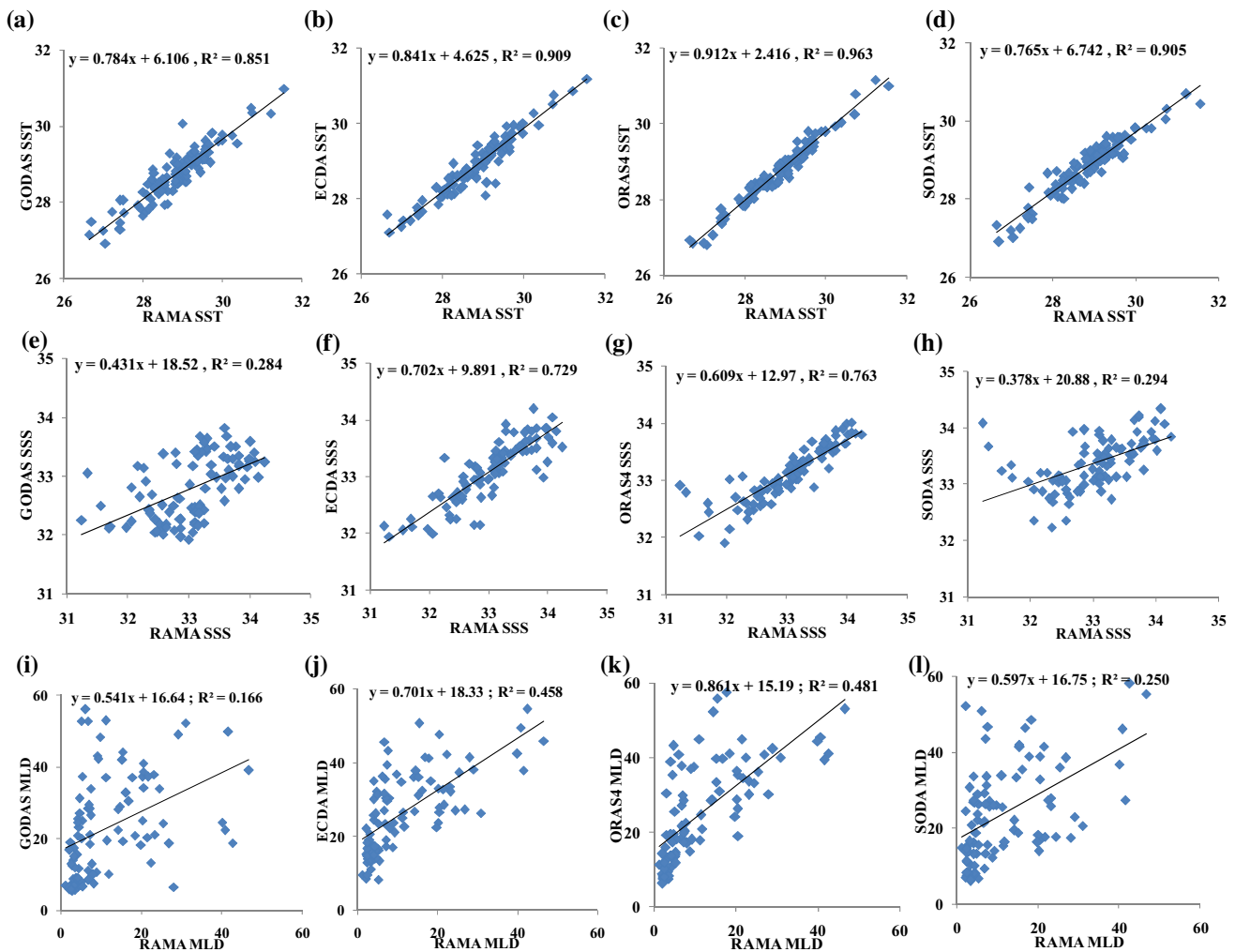
Fig. 12 Scatter plots of RAMA buoys observations against the reanalyses data for **a–d** SST (°C), **e–h** SSS and **i–l** MLD (m) from BoB region

Study explores the spatial and temporal evolution of differences/biases and RMSE in the upper ocean of the TIO. It is important to note that the reanalyses data sets are based on different ocean models constrained by different data assimilation methodology or strategies. Since these products are widely used for the various coupled model based temporal scale forecast and to understand oceanic phenomenon, the detailed assessment of their performance over the TIO is mandatory. This has motivated the present study to evaluate the status of mean spatial features in these reanalyses as well as explore the vertical structure of temperature, salinity and density with the insitu observations. Apart from the mean field assessment, temporal evolution of reanalyses with EN4 analysis and RAMA buoys observations are also carried out. Further the variability of surface oceanic variable over the TIO in EN4 analysis and all reanalyses data for the period of 1980–2010 is also examined. Upper ocean currents are evaluated with respect to satellites based OSCAR current observations.

All the reanalyses products display dominant warm bias in SST with the exception of GODAS. The strength of the SST biases is higher in south of the equator. Statistical analysis reveals that ORAS4 displays least RMSE in temperature fields followed by SODA, GODAS, and ECDA. The large differences between ECDA and the SST estimates of HadISST and Reynolds is undoubtedly due to the coupled nature of ECDA, whereas the other three reanalyses are heavily constrained by restoring to SST observations or analysis. Further, ORAS4 contains low RMSE and highest pattern correlation in SSS fields with respect to EN4 analysis. It is important to note that ORAS4 consists of five ensemble members and systematic ocean model biases are minimized in ORAS4 using observations rather than climatology fields. Higher positive SSS differences is reported in the north BoB and south eastern AS in all the reanalyses products. GODAS displays maximum SSS RMSE in the BoB compared to the other reanalyses, which could be arising due to the assimilation of synthetic salinity profiles rather than actual salinity

profiles. Synthetic salinity profiles are computed for each temperature profile using a local T–S climatology based on the annual mean fields of temperature and salinity from the NODC World Ocean Database. It is important to note that ECDA uses most advanced data assimilation technique with coupled model configuration whereas rest of the reanalyses products are based on standalone ocean models with data assimilation unit. SODA (GODAS) displays lowest (highest) RMSE in MLD, over the TIO. Dominant eastward current in the EIO is simulated by all the reanalyses however GODAS, ECDA, and SODA display westward bias. Statistical scores reveal that all the reanalyses display higher RMSE with weaker pattern correlation for the EIO circulation, whereas the representation of circulation is more realistic over rest of the TIO in all reanalyses. ORAS4 could capture equatorial current system better compared to other reanalyses. This could be due to assimilation of along track altimeter observations apart from assimilating T and S profiles (Balmaseda et al. 2013). Upper ocean stability and vertical shear analysis conclude that upper ocean stability is underestimated in all reanalyses. This is leading to excess mixing, which in turn leads to deeper MLD. Additional analysis suggests that salinity biases are mainly responsible for the upper ocean density biases, leading to weaker density gradient in all reanalyses (weakest in GODAS) consistent with the weaker stability. The better performance of ORAS4 in terms of density bias might be due to better performance of T/S balance operators utilized in that reanalysis. Temporal evolution of RMSE in GODAS reveals that SST and MLD RMSE peak during spring and summer. Ocean states during these months are crucial for seasonal and extended range prediction of the ISMR. Further SST, SSS, MLD variability assessment reveals that all the reanalyses overestimate the variability over the TIO with respect to EN4 analysis. RMSE estimates based on EN4 analysis/OSCAR indicate that RMSE in SSS, MLD and circulations are higher or equal to the variability strength of respective variable with the exception of SST. Error for all the above discussed parameters are also estimated with respect to RAMA buoys observations over the EIO and BoB. This analysis reveals that the error in MLD (SST) is higher (lower) than that based on EN4 analysis. Overall ORAS4 displays minimum error and maximum correlation with EN4 analysis as well as RAMA buoys. This could be due to assimilation of altimeter seal level data, ensemble-generation procedure and model bias-correction scheme in ORAS4, which are not there in other reanalyses. This study concludes that to improve the skill of the reanalyses in the TIO, the vertical structure of salinity needs to be improved and secondly reduce the excess vertical shear of the horizontal currents. Apart from these it is also important to improve precipitation, evaporation as well as river runoff forcing specifically to represent the BoB state in these reanalyses.

References

Adler RF, Huffman GJ, Chang A, Ferraro R, Xie PP, Janowiak J, Rudolf B, Schneider U, Curtis S, Bolvin D, Gruber A, Susskind J, Arkin P, Nelkin E (2003) The version-2 global precipitation climatology project (GPCP) monthly precipitation analysis (1979–present). J of Hydrometeorol 4(6):1147–1167

Agarwal N, Sharma R, Parekh A, Basu S, Sarkar A, Agarwal VK (2012) Argo observations of barrier layer in the tropical Indian Ocean. Adv Space Res 50:642–654. doi:10.1016/j.asr.2012.05.021

Antonov JI, Locarnini RA, Boyer TP, Mishonov AV, Garcia HE (2006) World ocean atlas 2005, vol 2. In: Levitus S (ed) Salinity, NOAA atlas NESDIS, vol 62. NOAA, Silver Spring

Balmaseda MA, Mogensen K, Weaver AT (2013) Evaluation of the ECMWF oceanreanalyses system ORAS4. Q J R Meteorol Soc 139:1132–1161

Balmaseda MA, Hernandez F, Storto A, Palmer MD, Alves O, Shi L, Smith GC, Toyoda T, Valdivieso M, Barnier B, Behringer D, Boyer T, Chang YS, Chepurin GA, Ferry N, Forget G, Fujii Y, Good S, Guinehut S, Haines K, Ishikawa Y, Keeley S, Köhl A, Lee T, Martin M, Masina S, Masuda S, Meyssignac B, Mogensen K, Parent L, Peterson KA, Tang YM, Yin Y, Vernieres G, Wang X, Waters J, Wedd R, Wang O, Xue Y, Chevallier M, Lemieux JF, Dupont F, Kuragano T, Kamachi M, Awaji T, Caltabiano A, Wilmer-Becker K, Gaillard F (2015) The ocean reanalyses inter-comparison project (ORA-IP). J Oper Oceanogr sup 1, s80–s97. doi:10.1080/1755876X.2015.1022329

Boyer TP, Antonov JI, Baranova OK, Garcia HE, Johnson DR, Locarnini RA, Mishonov AV, Seidov D, Smolyar IV, Zweng MM (2009) Chap. 1: introduction, NOAA atlas NESDIS 66. In: Levitus S (ed) World ocean database 2009, U.S. Gov. Printing Office, Washington, DC

Carton JA, Giese BS (2008) A reanalyses of ocean climate using simple ocean data assimilation (SODA). Mon Weather Rev 136:2999–3017. doi:10.1175/2007MWR1978.1

Chakravorty S, Chowdary JS, Gnanaseelan C (2014) Epochal changes in the seasonal evolution of tropical Indian Ocean warming associated with El Niño. Clim Dyn 42:805–822. doi:10.1007/s00382-013-1666-3

Chakravorty S, Gnanaseelan C, Pillai PA (2016) Combined influence of remote and local SST forcing on Indian summer monsoon rainfall variability. Clim Dyn. doi:10.1007/s00382-016-2999-5

Chattopadhyay R, Rao SA, Sabeerali CT, George G, Rao DN, Dhakate A, Salunke K (2015) Large-scale teleconnection pattern of Indian summer monsoon as revealed by CFSv2 retrospective seasonal forecast runs. Int J Climatol. doi:10.1002/joc.4556

Chowdary JS, Parekh Anant, Srinivas G, Gnanaseelan C, Fousiya TS, RashmiKhandekar, Roxy MK (2016) Processes associated with the tropical Indian Ocean subsurface temperature bias in a coupled model. J Phys Oceanogr. doi:10.1175/JPO-D-15-0245.1

Courtier P, Thépaut J-N, Hollingsworth A (1994) A strategy for operational implementation of 4D-Var, using an incremental approach. Q J R Meteorol Soc 120:1367–1388

Delworth TL, Rosati A, Stouffer RJ et al (2006) GFDL's CM2 global coupled climate models. part I: formulation and simulation characteristics. J Clim 19:643–674

Derber J, Rosati A (1989) A global oceanic data assimilation system. J Phys Oceanogr 19:1333–1347

Fousiya TS, Parekh A, Gnanaseelan C. 2015. Interannual variability of upper ocean stratification in Bay of Bengal: observational and modeling aspects. Theor Appl Climatol. doi:10.1007/s00704-015-1574-z

Gadgil S, Joseph PV, Joshi NV (1984) Ocean atmosphere coupling over monsoon regions. Nature 312:141–143

Gandin LS (1965) Objective analysis of meteorological fields. Israel Program for Scientific Translation, Jerusalem, p 242

Gnanaseelan C, Deshpande A, McPhaden MJ (2012) Impact of Indian Ocean dipole and El Niño/Southern oscillation forcing on the Wyrtki jets. J Geophys Res 117:C08005. 10.1029/2012JC007918

Good SA, Martin MJ, Rayner NA (2013) EN4: quality controlled ocean temperature and salinity profiles and monthly objective analyses with uncertainty estimates. J Geophys Res Oceans 118:6704–6716. doi:10.1002/2013JC009067

Gouretski V, Reseghetti F (2010) On depth and temperature biases in bathythermograph data: development of a new correction scheme based on analysis of a global ocean database. Deep Sea Res I 57:812–833. doi:10.1016/j.dsr.2010.03.011

Hosoda S, Ohira T, Sato K, Suga T (2010) Improved description of global mixed-layer depth using argo profiling floats. J Oceanogr 66(6):773–787. doi:10.1007/s10872-010-0063-3 2010.

Huang B, Xue Y, Zhang D, Kumar A, McPhaden MJ (2010) The NCEP GODAS ocean analysis of the tropical Pacific mixed layer heat budget on seasonal to interannual time scales. J Clim 23:4901–4925. doi:10.1175/2010JCLI3373.1

Ingleby B, Huddleston M (2007) Quality control of ocean temperature and salinity profiles—historical and real-time data. J Mar Syst 65:158–175

Kalnay E, Kanamitsu M, Kirtler R, Collins W, Deaven D, Gandin L, Iredell M, Saha S, White G, Woollen J, Zhu Y, Chelliah M, Ebisuzaki W, Higgins W, Janowiak J, Mo KC, Ropelewski C, Wang J, Leetma A, Reynolds R, Jenne R, Joseph D (1996) The NCEP/NCAR 40-year reanalysis project. Bull Am Meteorol Soc 77:437–471

Kanamitsu M, Ebisuzaki W, Woollen J, Yang SK, Hnilo JJ, Fiorino M, Potter GL (2002) The NCEP-DOE AMIP-II reanalysis (R-2). Bull Am Meteorol Soc 83:1631–1643

Liu L, Xie S-P, Zheng X-T, Li T, Du Y, Huang G, Yu WD (2014) Indian Ocean variability in the CMIP5 multi-model ensemble: the zonal dipole mode. Clim Dyn 43:1715–1730. doi:10.1007/s00382-013-2000-9

Locarnini RA, Mishonov AV, Antonov JI, Boyer TP, Garcia HE, 2006. World ocean atlas 2005, vol 1: temperature. In: Levitus S (ed) NOAA atlas NESDIS 61. U.S. Government Printing Office, Washington, DC

Madec G, 2008. NEMO ocean general circulation model reference manuel. Internal report. LOCEAN/IPSL, Paris

McPhaden MJ et al (2009) The research moored array for African–Asian–Australian monsoon analysis and prediction. Bull Am Meteorol Soc RAMA:459–480

Mogensen K, Balmaseda MA, Weaver A (2012) The NEMOVAR ocean data assimilation system as implemented in the ECMWF ocean analysis for system 4. ECMWF Tech Memo, Reading **(668)**

Nyadjro E, McPhaden MJ (2014) Variability of zonal currents in the eastern equatorial Indian Ocean on seasonal to interannual time scales. J Geophys Res Oceans 119:7969–7986. doi:10.1002/2014JC010380

Palmer MD, Roberts CD, Balmaseda M, Chang YS, Chepurin G, Ferry N, Fujii Y, Good SA, Guinehut S, Haines K, Hernandez F, Köhl A, Lee T, Martin MJ, Masina S, Masuda S, Peterson KA, Storto A, Toyoda T, Valdivieso M, Vernieres G, Wang O, Xue Y (2015) Ocean heat content variability and change

in an ensemble of ocean reanalyses. Clim Dyn. doi:10.1007/s00382-015-2801-0

Rayner NA, Parker DE, Horton EB, Folland CK, Alexander LV, Rowell DP, Kent EC, Kaplan A (2003) Global analyses of sea surface temperature, sea ice, and night marine air temperature since the late nineteenth century. J Geophys Res 108(D14):4407. doi:10.1029/2002JD002670

Reynolds RW, Rayner NA, Smith TM, Stokes DC, Wang W (2002) An improved in situ and satellite sst analysis for climate. J Clim 15:1609–1625

Saha S, Nadiga S, Thiaw C, Wang J, Wang W, Zhang Q, van den Dool HM, Pan H-L, Moorthi S, Behringer D, Stokes D, Peña M, Lord S, White G, Ebisuzaki W, Peng P, Xie P (2006) The NCEP climate forecast system. J Clim 19:3483–3517

Saha S et al (2014) The NCEP climate forecast system version 2. J Clim 27:2185–2208. doi:10.1175/JCLI-D-12-00823.1

Saji NH, Yamagata T (2003a) Possible impacts of Indian Ocean dipole mode events on global climate. Clim Res 25:51–169

Saji NH, Yamagata T (2003b) Structure of SST and surface wind variability during Indian Ocean dipole mode years: COADS observations. J Clim 16:2735–2751

Saji NH, Goswami BN, Vinayachandran PN, Yamagata T (1999) A dipole mode in the tropical Indian Ocean. Nature 401:360–363

Sayantani O, Gnanaseelan C (2015) Tropical Indian Ocean subsurface temperature variability and the forcing mechanisms. Clim Dyn 44:2447–2462

Schott F, McCreary JP (2001) The monsoon circulation of the Indian Ocean. Prog Oceanogr 51:1–123

Schott F, Dengler M, Schoenefeldt R (2002) The shallow thermohaline circulation of the Indian Ocean. Prog Oceanogr 53:57–103

Schott FA, Xie S-P, McCreary JP Jr (2009) Indian Ocean circulation and climate variability. Rev Geophys 47:RG1002. doi:10.1029/2007RG000245

Seetaramayya P, Master A (1984) Observed air–sea interface conditions and a monsoon depression during MONEX-79. Meteorol Atmos Phys 33:61–67

Sengupta D, Goswami BN, Senan R (2001) Coherent intraseasonal oscillations of ocean and atmosphere during the Asian summer monsoon. Geophys Res Lett 28:4127–4130

Shenoi SSC, Shankar D, Shetye SR (2002) Differences in heat budgets of the near-surface Arabian Sea and Bay of Bengal: implications for the summer monsoon. J Geophys Res 107:3052. doi:10.1029/2000JC000679

Shetye SR, Gouveia AD, Shenoi SSC, Vinayachandran PN, Sundar D, Michael GS, Nampoothiri G (1996) Hydrography and circulation in the western Bay of Bengal during the northeast monsoon. J Geophys Res 101:14011–14025

Shi L, Alves O, Wedd R, Balmaseda MA, Chang Y, Chepurin G, Ferry N, Fujii Y, Gaillard F, Good SA, Guinehut S, Haines K, Hernandez F, Lee T, Palmer M, Peterson KA, Masuda S, Storto A, Toyoda T, Valdivieso M, Vernieres G, Wang X, Yin Y (2015) Anassessment of upper ocean salinity content from the ocean reanalyses inter-comparison project (ORA-IP). Clim Dyn. doi:10.1007/s00382-015-2868-7

Shukla J (1975) Effect of arabian sea-surface temperature anomaly on Indian summer monsoon: a numerical experiment with the GFDL model. J Atmos Sci 32:503–511

Sikhakolli R, Rashmi S, Basu S, Gohil BS, Sarkar A, Prasad KVSR (2013) Evaluation of OSCAR ocean surface current product in the tropical Indian Ocean using in-situ data. J Earth Syst Sci 122(1):187–199

Smith RD, Dukowicz JK, Malone RC (1992) Parallel ocean general circulation modeling. Physica D 60:38–61

Taylor KE, Stouffer RJ, Meehl GA (2012) An overview of CMIP5 and the experiment design. Bull Am Meteorol Soc 93(4):485–498. doi:10.1175/BAMS-D-11-00094.1

Toyoda T, Fujii Y, Kuragano T, Kamachi M, Ishikawa Y, Masuda S, Sato K, Awaji T, Hernandez F, Ferry N, Guinehut S, Martin MJ, Peterson KA, Good SA, Valdivieso M, Haines K, Storto A, Masina S, Khl A, Zuo Hao, Balmaseda M, Yin Y, Shi L, Alves O, Smith G, Chang Y, Vernieres G, Wang X, Forget G, Heimbach P, Wang O, Fukumori I, Lee T (2015) Intercomparison and validation of the mixed layer depth fields of global ocean syntheses. Clim Dyn. doi:10.1007/s00382-015-2637-7

Webster PJ, Moore AM, Loschnigg JP, Leben RR (1999) Coupled ocean–atmosphere dynamics in the Indian Ocean during 1997–98. Nature 401:356–360

Weller RA, Farrar JT, Buckley J, Mathew S, Venkatesan R, SreeLekha J, Chaudhuri D, Suresh Kumar N, Praveen Kumar B (2016) Air–sea interaction in the Bay of Bengal. Oceanography 29(2):28–37. doi:10.5670/oceanog.2016.36

Wyrtki K (1973) An equatorial jet in the Indian Ocean. Science 181:262–264

Xie SP, Hu K, Hafner J, Tokinaga H, Du Y, Huang G, Sampe T (2009) Indian Ocean capacitor effect on Indo–western Pacific Climate during the summer following El Niño. J Clim 22:730–747

Zhang S, Rosati A (2010) An inflated ensemble filter for ocean data assimilation with a biased coupled GCM. Mon Weather Rev 138:3905–3931. doi:10.1175/2010MWR3326.1